Dear Dr. Teuling,

Please find attached our revised manuscript, “Data-driven estimates of evapotranspiration and its controls in the Congo Basin” (HESS-2020-186). Thanks to the insightful comments of our two reviewers, we believe the manuscript is much strengthened and will serve as a valuable contribution to the growing body of literature on the hydrology of the Congo River Basin.

While the structure and central narrative of the paper remain essentially unchanged, we have strengthened several components of the article at the suggestion of our reviewers. We now include the energy balance and remote sensing-based SSEBop product into our analysis of global ET products, based on Reviewer 1’s suggestion to include global ET products that a recent pan-African study found to be most accurate in the Congo Basin. Reviewer 2 suggested additional metrics for comparing the seasonal cycles of global ET products; we have added these metrics into our Results and Discussion sections as well. Reviewer 2 also prompted us to include more discussion of within-basin spatial variability, previous phenological studies, and PAR normalization of SIF data (for which we have also added an additional figure to the Supplement). Both reviewers wrote that additional perspective on research needs/opportunities would be welcome in the article, and to this end we have added two new paragraphs (one in its own new subsection) to the Discussion section. Numerous other technical details and clarifications have been added throughout the text, and we also slightly reworded the title to sound less redundant.

In addition to the changes brought about by our discussions with reviewers, we made two technical corrections to the article to address errors we uncovered after the initial submission. Comparing our results to recent literature cited by Reviewer 1 led us to realize that our Congo Basin ET data from GLEAM v3.1 and MOD16A2 were erroneously low due to mistakes in processing the data. We have corrected these mistakes and also taken the opportunity to update our data to the more recent GLEAM v3.3 product. While we made significant changes to the text of Sections 3.3 and 4.3 to correctly reflect the performance of the GLEAM and MOD16A2 products, our primary conclusions regarding the failure of global ET models to capture the variability of ET in the Congo remain essentially unchanged. Finally, we noticed that one subplot in the previous version of our manuscript (Fig. 7c) was displaying PAR data without the mean seasonal cycle removed, as was reported in the caption; this error has been fixed and again had no impact on the findings of the article.

We believe we have sufficiently addressed the thoughtful concerns of our reviewers, and that the messages of our article are clearer and more thorough as a result. A point-by-point response to our reviewers’ comments is included alongside the marked-up revision of our article.

Sincerely,

Michael W. Burnett

Gregory R. Quetin

Alexandra G. Konings

Response to Reviews – Burnett et al. (HESS-2020-186)

Reviewer 1:

> ***Referee Comment:*** *This study produces a monthly basin-wide ET estimates for the Congo basin based on the water balance approach for the period April 2002 to December 2016 evaluated against previous literature estimates and six global ET products. Drivers were investigated for the seasonal and interannual variability. This study is very well structured and written, with a good flow and ease to read and understand the concepts being used. The author has been thorough in his review of existing studies, making good comparisons and analyses to their findings throughout the paper. I have a few minor comments as follows.*

Author Response: We are glad the reviewer took a positive view of the article. Responses to comments are included below.

> ***Referee Comment:*** *It would be interesting if you could discuss whether the use of this technique can be easily applied to other basins even without the use of a precipitation product being developed specifically for a particular basin under study? The findings are very interesting and can be useful for other larger basins in Africa such as the Niger basin with a large delta and the Nile basin.*

Author Response: In the revised draft we have added the following text in discussion section 4.1 regarding this topic:

"The results of this study also reinforce the value of the inverted water balance method for studying river basins large enough to accommodate the coarse spatial resolution of GRACE data. Compared to the difficulty of directly measuring ET and the large amount of observational data needed to constrain ET models, the inverted water balance is conceptually straightforward and has relatively simple data requirements. But as demonstrated here and in other large river basins like the Amazon (Maeda et al., 2017; Swann and Koven, 2017), inverting the water balance produces robust estimates of ET which can be used to validate and improve other ET models' representation of sparsely-observed basins. Limitations of water balance ET estimates include the coarse spatial resolution, monthly timesteps, and short temporal coverage of GRACE (2002–2016, with various data gaps), the availability of river discharge data for the area of interest, and the quality of gridded *P* data in the region. However, the use of *dS/dt* data may not be necessary in long-term ET estimates (Weerasinghe et al. 2020), so the limitations of GRACE data mostly affect studies examining ET variability on annual or shorter timescales. The uncertainties of *P* datasets can be assessed and mitigated using techniques such as TC (Stoffelen 1998; McColl et al., 2014; Alemohammad et al. 2015; Dong et al. 2020), but basins with more thorough gauge coverage than the Congo probably do not require such detailed analysis of multiple gridded *P* products."

> ***Referee Comment:*** *You compare the ETwb with six available global ET products. As I see you have referenced Weerasingle et al., that also found that GLEAM and MOD16A2 were*

substantially underestimating ET at the long-term annual scale, whereas other products within that study had much lower biases. It would be interesting to see the same comparison with one or more of the products with lower biases in their study to see if those products capture the seasonal variations and bias better than the products being analysed in this study.

Author Response: In the revised paper we have included SSEBop as a seventh global ET product for comparison, as it is the global product recommended by Weerasinghe et al. with the lowest bias over the Congo Basin and the most use in the literature.

Referee Comment: *P3L65 – you say that studies assume no change in water storage when applying the water balance equation and state 'an assumption with little support'. Is this really true? In the study previously mentioned, Weerasinghe et al., they have looked at the largest contribution of the change in annual water storage from a study using GRACE data and found this to be 20mm yr-1. They then applied this to several basins in Africa including the Congo basin and found there to be only a 2.3% representation of total long-term annual average ET. I believe this assumption has been made for large watersheds and for long-term averages and there is actually a lot of existing studies to support this. Be careful with this statement. Also, In all studies, if it is possible to use the change in storage, this should always give better results, although it may be negligible depending on the timescale and size of area and thus may not be the most important aspect of their studies if not looking at smaller temporal and spatial scales.*

Author Response: This is a good point. We agree that the language in the previous version of our manuscript may be too strong, although we do maintain the importance of incorporating terrestrial water storage changes in water balance estimates of ET at monthly timescales. We have revised the paragraph to read as follows:

"While some previous studies have applied a similar technique to the Congo Basin as part of larger-scale experiments, these studies assumed terrestrial water storage was constant over their study periods (Marshall et al., 2012; Ukkola and Prentice, 2013; Weerasinghe et al., 2020)—a plausible assumption for long-term ET estimates, but one that could mask a large degree of ET variability on annual and shorter timescales. Indeed, remotely-sensed evidence suggests water storage anomalies within the basin do change significantly on a monthly and interannual basis (Crowley et al., 2006; Rodell et al., 2018), even if long-term trends are typically small relative to the magnitude of ET fluxes (Weerasinghe et al., 2020). Thus in order to explore seasonal cycles and variations in basin-wide ET, terrestrial water storage must be constrained in inverted water balance models…"

Referee Comment: *P1L10 – '…second-largest river basin in the world…'*

Author Response: Corrected in revised manuscript.

Referee Comment*: Table 1 caption has 'in' twice consecutively.*

Author Response: Corrected in revised manuscript.

> ***Referee Comment:*** *P14L355 – I would mention here the three variables you are considering in the text so the reader does not have to go to the figure before they know.*

Author Response: The clarification on P14L355 has been added to the text, thank you.

Reviewer 2:

> ***Referee Comment:*** *This article presents (1) the development of evapotranspiration estimate for the whole of the Congo Basin based on a water balance equation where components are either derived from up-to-date satellitate estimates (P, ds/dt) or in-situ measurements (Q, P), (2) a comparison with 6 existing products developed at global scale from different sources (model, reanalyses, satellites, in-situ) and (3) an analysis of the drivers of ET variations at the mean annual and interannual scale.*
>
> *I find the article particularly well written and structured, with a carefull use of the multiple databases selected for analysis and interesting discussion sections regarding the drivers. A lot of the papers cited are also quite recent ones so that this paper itself is a nice review of the last findings for the CB. It is also particularly relevant as the functionning and inter-relationships of the hydrologic, biospheric and climatic components of the Congo Basin are far less well known and documented than those of Amazonia. An interesting finding is the potential role of the radiative forcing.*

Author Response: We are glad the referee took a positive view of the article.

> ***Referee Comment:*** *L125 : amongst the quite recent and few attempts of rainfall estimates validation against in-situ measurements for CB you could also refer to Camberlin et al 2019 QJRMS*

Author Response: Camberlin et al. (2019) is now cited several times throughout the study.

> ***Referee Comment:*** *L247 : I would specify here « correlation at the interannual time-scale » (and not for the mean annual cycles)*

Author Response: This line is clarified in the revised article. The sentence now states: "In order to track interannual correlations between ET_{wb}, meteorological variables, and vegetation indices, the Breaks for Additive Season and Trend (BFAST) R package (Verbesselt et al., 2015) was used…"

> ***Referee Comment:*** *Fig1 + all your figures : would be very helpful to readers if gridlines were provided so that we can better pick the peaks and lows, the lead-lags between variables etc*

Author Response: We have added gridlines to all figures in the paper, although horizontal gridlines are omitted where multiple y-axes are used in single plots, and vertical gridlines are omitted in Figs. 6 and 7 to preserve the visual clarity of the figures. Since the data in these plots will be made available to interested scholars in an online repository after publication (http://doi.org/10.17605/OSF.IO/JPVMB), we believe the gridlines we added will be sufficiently useful for conveying our messages in the text.

Referee Comment: *L286 : part of the discussion about the shape of the mean annual cycle with a minima in JJA being driven by the southern pixels (which are dominant in the CB, e.g. L360) should appear as soon as this section*

Author Response: Thank you, this is a good point. This paragraph now begins, "Plotting monthly means of the water balance fluxes provides further clarity regarding their seasonal cycles (Fig. 2). The basin-wide seasonal flux cycles are dominated by contributions from the region south of the equator, which comprises the majority of the Congo Basin (Fig. S2)."

Referee Comment: *L289 : to me when reading the figure the fastest S decrease is between April and May …*

Author Response: Fig. 2 plots *dS/dt* rather than *S*. While *dS/dt* decreases the fastest between April and May, *S* does not. To clarify, we have revised this paragraph to include "Positive *dS/dt* rates indicate *S* regenerates mostly during the very wet October and November months…".

Referee Comment: *L308-311 : these differences in terms of dynamics, amplitude and ratio between MAM and SON are an important point that certainly plays then on the analysis of drivers … your ET estimate is singular from this point of view. you might provide these two statistics (amplitude, ratio) to support your discourse …*

Author Response: We have added these statistics into Table 3 and included discussion of amplitude and ratio in Section 3.3.

Referee Comment: *Table 3 : why don't you provide the annual mean on 2002-2011 if you compute correlations etc on this period ??? You should also provide the significance level for the correlations …*

Author Response: We had previously used a different annual mean averaging period to avoid using data-incomplete years (which would bias the annual mean ETs), but we agree that this was confusing. Since we have added a comparison to SSEBop in the revised manuscript (based on Reviewer 1's recommendation), we now evaluate all metrics and averages on the 2003-2011 period anyways, so this issue has been solved.

Referee Comment: *L346 : could you explain a bit the added value of normalising SIF by PAR*

Author Response: Normalizing SIF by PAR is intended to isolate the contributions of climatic and ecophysiological factors to productivity while controlling for the influence of radiation on productivity. This was designed to allow us to read clearer information about moisture availability, light use efficiency, and vegetation dynamics from the SIF data. We have added a sentence to Section 2.4 to clarify this point and to reference recent studies that did the same: "SIF was normalized by monthly CERES total PAR data in order to isolate the effects of phenological, physiological, and hydrological

variability on plant productivity independent of radiative controls (Madani et al., 2017; Pagán et al., 2019)."

The relatively low variance of total PAR also means that the SIF seasonal cycle and peak during October/November are similar with and without PAR normalization (see the new Supplemental Figure S3). Text has been added to Section 3.4 to note this: "SIF peaks in October and November with or without PAR normalization (Fig. S3), indicating both greater total photosynthesis and more light-efficient production during these months". In addition, we have further leveraged our use of PAR-normalized SIF in Section 4.2, noting evergreen forest LUE appears to be greater in SON than in MAM.

> ***Referee Comment:*** *L352 : I dont' think that the ratio is « significantly » greater in SON as compared to MAM as the greatest ratio is observed in May ; it seems quite comparable (and easy to check) so to my opinion this does not play ...*

Author Response: It is true that in terms of seasonal means they are not much different. In the revised line we clarify that March and April have low diffuse PAR ratios that could cause the high ET observed in those months (in May, when diffuse PAR ratio peaks, ET decreases to nearly SON levels):

"WUE during SON may be higher than in March and April (when ET_{wb} peaks) because of the greater ratio of diffuse PAR to total PAR during SON (Fig. 4d) which can increase photosynthetic efficiency (Mercado et al., 2009), as further discussed in Sect. 4.2.3."

> ***Referee Comment:*** *L371 : the positive trend in radiation might not be a regional signal only as many studies have shown a brightening at global scale the past decade (as opposed to a dimming in the 90s)*

Author Response: This is a good point. We tried to add text related to this point to the manuscript, but dimming/brightening trends in central Africa do not seem well-constrained during our study period in the literature, and we ultimately found there was no succinct way to summarize the relevant point without distracting from the message of the paragraph, which is about how different trends in drivers combine to influence ET trends. Thus, for the sake of clarity of the remaining message, and because it does not affect our interpretation, we have not incorporated it here.

> ***Referee Comment:*** *L400 : the scale of your study is far larger than the ones by Betbeder et al and Philippon et al which focus on very specific forests growing on particular soils, therefore I would not be so affirmative about a unique and consistant peak of EVI in SON across the whole central Africa forests even if these authors have not used the last state of the art EVI product...*

Author Response: This is a good point—we have added text to this section noting the smaller extent of the Betbeder and Philippon studies as a likely cause of the different EVI cycles, and to clarify that the different EVI algorithms used are merely an additional factor on top of the spatial differences:

"However, these studies focused on specific areas of evergreen forests and wetlands that may not represent the ecohydrology of the Congo Basin's entire equatorial rainforest belt, and used MODIS

products that do not fully account for sun-sensor geometry and other sources of error at low latitudes (Hilker et al., 2012; Bi et al., 2016)."

> ***Referee Comment:*** *4.2.4 water storage : Your discussion is valid for southern pixels but not the northern ones … while the wettest rainy season is SON over the whole CB, the driest rainy season is DJF to the north and JJA to the south so this changes the dynamics of water storage and available water for trees at the beginnign of each rainy season ...*

Author Response: This is true—section 4.2.4 has been modified to clarify that much of the discussion pertains to the southern portion of the basin, but that the hydrologic characteristics of the southern region dominate the basin-wide hydrologic cycles and are therefore still relevant to the study:

"As with other variables examined in this study, seasonal *S* dynamics at the basin scale are driven by the wet SON and dry JJA seasons experienced by the larger southern portion of the basin. Even though basin-wide *P* during MAM is significant, *dS/dt* (which measures groundwater within the rooting zone as well as in deeper reserves) remains much lower than its SON levels and only seems to recharge *S* enough to compensate for the slightly negative *dS/dt* values of January and February (Fig. 2), indicating that water reserves are largely saturated during MAM and undersaturated at the onset of SON when averaged across the basin (Fig. 4f). This hypothesis is consistent with prior soil moisture modeling efforts, which indicate that Congolese ecosystems south of the equator (i.e. most of the basin's area) feature low soil moisture as SON rains begin before maintaining high soil moisture and deeper water reserves through the end of the MAM rainy season (Pokam et al., 2012; Guan et al., 2014)."

> ***Referee Comment:*** *L540 : I would also add, amongst the reasons why you do not capture the negative trend in rainfall, that this trend mainly affects the northern part of the CB and your index is mainly « driven » by southern pixels*

Author Response: Thanks for the suggestion - we added the spatial mismatch to the list of reasons presented in this line, along with two references on the northern bias in rainfall declines:

"However, the absence of a trend in P_{TC} does not prove the absence of a longer-term drying trend that began in the 20th century—rather, it probably results from our study period, which is shorter and generally more recent than those of the aforementioned studies, our analysis of rainfall over all seasons rather than during certain three-month windows, and the fact that rainfall declines mainly affect the northern portion of the basin (Zhou et al., 2014; Hua et al., 2016) whereas our study is dominated by the basin area south of the equator (Fig. S2)."

> ***Referee Comment:*** *Fig.2S : would be good that the CB be contextualised ie by presenting a larger map of Central Africa with countries borders ....*

Author Response: We have added a geopolitical map with Congo Basin boundaries as an additional panel in Figure S2.

Referee Comment: *Lastly I would have liked seeing in this paper a short « perspective » section on the further analyses these results call for and the study limits (unfortunately ET at the monthly and CB scale that does not allow documenting spatial variations in the drivers of ET that might be significant nor fine temporal - daily or infra-daily – variations which might be key to understand differences between the two wet or the two dry periods)*

Author Response: We added a "Section 4.5: Opportunities for further study" to the end of the Discussion outlining some further analyses that would be useful. It reads:

"This study demonstrates the value in combining in-situ observations with remote sensing in data-sparse regions like the Congo Basin. However, there are clear limitations to the water-balance approach employed here that suggest several opportunities for further study of the region. For instance, applying the inverted water balance model at the basin scale masks differences in the magnitude and variability of ET across the diverse regions of the Congo Basin, yet the availability of river discharge data from tributaries of the Congo River could allow for modeling of ET at the sub-basin scale (Alsdorf et al., 2016). Similarly, the monthly temporal resolution of the GRACE data prevents examination of diurnal and sub-monthly variations in ET. While GRACE data also represent a relatively short time span, the GRACE Follow-On (GRACE-FO) mission promises to extend the global *S* dataset well into the future. Ultimately, improved in-situ observations of hydrologic and climatic fluxes are necessary to understand the ecohydrology of central Africa in greater detail and at finer scales—eddy covariance towers, weather stations, and long-term phenological surveys would all be of great benefit to the growing field of research on the Congo Basin."

Data-driven estimates of evapotranspiration and its ~~drivers~~ controls in the Congo Basin

Michael W. Burnett[1], Gregory R. Quetin[2], Alexandra G. Konings[2]

[1]Earth Systems Program, Stanford University, Stanford, CA, USA
[2]Department of Earth System Science, Stanford University, Stanford, CA, USA

Correspondence to: Michael W. Burnett (mburnett@alumni.stanford.edu)

Abstract

Evapotranspiration (ET) from tropical forests serves as a critical moisture source for regional and global climate cycles. However, the magnitude, seasonality, and interannual variability of ET in the Congo Basin remain poorly constrained due to a scarcity of direct observations, despite ~~it~~ the Congo being the second-largest river basin in the world and containing a vast region of tropical forest. In this study, we applied a water balance model to an array of remotely-sensed and in-situ datasets to produce monthly, basin-wide ET estimates spanning April 2002 to November 2016. Data sources include water storage changes estimated from the Gravity Recovery and Climate Experiment (GRACE) satellites, in-situ measurements of river discharge, and precipitation from several ~~remotely~~ remotely-sensed and gauge-based sources. An optimal precipitation dataset was determined as a weighted average of interpolated data by Nicholson et al. (2018), Climate Hazards Infrared Precipitation with Station Version 2 (CHIRPS2) data, and the Precipitation Estimation from Remotely Sensed Information using Artificial Neural Networks–Climate Data Record product (PERSIANN-CDR), with the relative weights based on the error magnitudes ~~in~~ of each dataset as determined by triple collocation. The resulting water balance-derived ET (ET_{wb}) features a long-term average that is consistent with previous studies (117.2±3.5 cm/year), but displays greater seasonal and interannual variability than ~~six~~ seven global ET products. The seasonal cycle of ET_{wb} generally tracks that of precipitation over the basin, with the exception that ET_{wb} is greater in March-April-May (MAM) than in the relatively wetter September-October-November (SON) periods. This pattern appears to be driven by seasonal variations in diffuse photosynthetically-active radiation (PAR) fraction, net radiation (R_n), and soil water availability. From 2002–2016, R_n, PAR, and vapor-pressure deficit (VPD) all increased significantly within the Congo Basin; however, no corresponding trend occurred in ET_{wb}. We hypothesize that the stability of ET_{wb} over the study period despite sunnier and less humid conditions may be due to increasing atmospheric CO_2 concentrations that offset the impacts of rising VPD and irradiance on stomatal water use efficiency (WUE).

1 Introduction

The Congo River Basin in central Africa is the second-largest river basin in the world and supports one of Earth's three major humid tropical forest regions (Alsdorf et al., 2016). Approximately 24 to 39 percent of evapotranspiration (ET) from the Congo

Basin is recycled as local rainfall (Dyer et al., 2017), and model simulations indicate changes in ET within the basin affect moisture cycling across the African continent (Van Der Ent and Savenije, 2011; Bell et al., 2015; Sorí et al., 2017). Understanding the magnitude, variability, and drivers of ET in the Congo Basin is therefore crucial for studying the climate systems of central Africa and the global tropics, especially because significant environmental shifts have already been reported within the basin. For instance, deforestation is an ongoing problem in Congolese forests~~,~~ with potential impacts on climate (Laporte et al., 2007; Batra et al., 2008; Bell et al., 2015; Turubanova et al., 2018); temperatures are rising due to anthropogenic climate change (Collins, 2011; James and Washington, 2013); and many have reported a long-term decline in precipitation over the basin (Asefi-Najafabady and Saatchi, 2013; Diem et al., 2014; Zhou et al., 2014; Hua et al., 2016; Dezfuli, 2017). Such shifts are particularly concerning because Africa's tropical rainforests are already significantly drier than other humid tropical forests and exist at the climatic threshold of conversion from evergreen to deciduous trees (Guan et al., 2015; Philippon et al., 2019; Bush et al., 2020).

However, the hydrology of the Congo Basin is vastly understudied relative to the region's size and influence (Alsdorf et al., 2016). In particular, no long-term observational studies of ET in the basin exist. There are also no eddy covariance towers operating within the Congo Basin. Prior studies provide only limited information and either analyze short-term ET observations at individual site scale (Nizinski et al., 2011, 2014) or rely on combining site scale meteorological measurements ~~at a site scale~~ with localized models (Bultot, 1971; Lauer, 1989; Shahin, 1994). Some studies have also used process-based models to evaluate regional ~~scale~~ ET (Matsuyama et al., 1994; Shem, 2006; Batra et al., 2008; Chishugi and Alemaw, 2009; Marshall et al., 2012; Ndehedehe et al., 2018; Crowhurst et al., 2020). However, the large size and heterogeneity of the Congo Basin render point-based approaches inadequate for basin scale analysis of hydrological cycling, and regional scale models suffer from being poorly constrained because of the widespread lack of in-situ observations throughout the basin (e.g. little understanding of local variability in rooting depth, vegetation responses to water and light availability, canopy interception, etc.). As a result, even basic seasonality patterns across the Congo Basin remain unclear. For example, Konings et al. (2017) showed that canopy water content increases during dry season, which could be due to either dry season leaf-out or a change in plant water uptake during the dry season that would increase ET. The latter could not be ruled out in Konings et al. (2017) due to the lack of direct ET estimates in the region.

Remote sensing offers a partial solution to this scarcity of ET observations. Remote sensing-based estimates of ET are generally indirect, relying on physical models to link temperature, meteorological inputs, and/or other observables to the rate of ET (Zhang et al., 2016). However, these modeling approaches are poorly constrained in the Congo River Basin and may be highly erroneous there. Alternatively, basin scale ET can be estimated indirectly by inverting the water balance. This approach requires only three geophysical input variables: precipitation, river discharge, and the change in terrestrial water storage. Precipitation and total water storage change can both be estimated using remote sensing, with the latter determined by gravity measurements from the Gravity Recovery and Climate Mission (GRACE) (Tapley et al., 2004; Swenson, 2012). Recent examples of this method's application include the Amazon Basin (Maeda et al., 2017; Swann and Koven, 2017) and the coterminous United States (Wan et al., 2015), as well as global examinations of basin scale ET (Liu et al., 2016).

While some previous studies have applied a similar technique to the Congo Basin as part of larger-scale experiments, these studies assumed terrestrial water storage was constant over their study periods (Marshall et al., 2012; Ukkola and Prentice, 2013; Weerasinghe et al., 2020)—a plausible assumption for long-term ET estimates, but one that could mask a large degree of ET variability on annual and shorter timescales~~n assumption with little support~~. Indeed, remotely-sensed evidence suggests water storage anomalies within the basin do change significantly on monthly and interannual timescales (Crowley et al., 2006; Rodell et al., 2018), even if long-term trends are typically small relative to the magnitude of ET fluxes (Weerasinghe et al., 2020). Thus in order to explore seasonal cycles and variations in basin-wide ET, terrestrial water storage must be constrained in inverted water balance models. In this paper, we applied the water balance method to the Congo Basin to produce the first data-driven estimates of monthly basin-averaged ET for the period from April 2002 to November 2016. To determine the most accurate precipitation time series to use in this computation, precipitation data from multiple remote sensing-based approaches was combined based on uncertainty ~~estimation~~ estimates from~~using~~ triple collocation. We further used the resulting ET time series to explore the climatic and ecological drivers of ET seasonality and trends by comparing it against a variety of vegetation indices and meteorological drivers.

2 Methods

Based on mass balance, any precipitation that falls on a basin and is not removed from the basin through river discharge or ET must increase the amount of water stored in the basin in the form of groundwater, soil moisture, or open water bodies. The equation for this mass balance can be rearranged to solve for ET as follows:

$$ET_{wb} = P - Q - \frac{dS}{dt} \quad (1)$$

where ET_{wb} is monthly basin-wide evapotranspiration, P is the monthly basin-wide precipitation, Q is total monthly runoff from the Congo River, S is the water storage anomaly within the basin expressed as an equivalent water height (Rodell et al., 2004a, 2011), and t is time. We calculate ET_{wb} using P from a combination of remotely-sensed and gauge-based precipitation products, as further discussed in Sects. 2.1 and 2.2. Q was obtained from a stream gauge at the outlet of the Congo River at Kinshasa-Brazzaville. Lastly, dS/dt was derived from the monthly change in terrestrial water storage throughout the basin, as estimated by gravitational anomaly data from GRACE (Tapley et al., 2004; Swenson, 2012).

2.1 Water balance data sources

The area and extent of the Congo Basin were determined using the 15-arcsecond HydroSHEDS Level 5 Basin Boundaries product (Lehner et al., 2008). The HydroSHEDS boundary produces a total basin area of 3,705,220 km^2—in good agreement with a recent independent estimate of 3,687,000 km^2 (Alsdorf et al., 2016). The HydroSHEDS product was used to trim all remotely-sensed raster data to the Congo Basin's boundaries at 0.01° spatial resolution (all datasets with coarser spatial resolutions mentioned hereafter were first resampled to 0.01° grids with no interpolation before determining their basin-wide values).

Basin-wide runoff (Q) for the Congo Basin was estimated using monthly discharge data collected from the Congo River at Kinshasa-Brazzaville. The long-running gauging station is operated by the Observation Service for Geodynamical, Hydrological and Biogeochemical Control of Erosion/Alteration and Material Transport in the Amazon, Orinoco and Congo Basins (SO-HYBAM) and captures the drainage of over 98% of the Congo Basin's area (Alsdorf et al., 2016). Because no uncertainty estimate is available for the streamflow gauge, we assumed an uncertainty range of ±20%.

Changes in terrestrial water storage (*dS/dt*) were calculated using *S* data from NASA's Gravity Recovery and Climate Experiment (GRACE) satellites (Swenson and Wahr, 2006; Landerer and Swenson, 2012; Swenson, 2012). In order to estimate monthly *S*, three independent GRACE solutions in 1° grids from Geoforschungs Zentrum Potsdam (GFZ), Jet Propulsion Laboratory (JPL), and the Center for Space Research at University of Texas, Austin (CSR) were retrieved. A scale factor grid was also applied to the GRACE data to account for attenuation of small-scale surface mass variations (Landerer and Swenson, 2012). The arithmetic mean of the three *S* solutions was used in the primary *dS/dt* calculation in order to reduce noise (Wahr et al., 2006; Sakumura et al., 2014), though all three independent *S* solutions were also used to calculate unique *dS/dt* values in order to estimate uncertainty in the GRACE products (Lee et al., 2011). The *S* data were converted to *dS/dt* values using a centered-difference approach at monthly timescale:

$$\frac{dS}{dt}_n = (S_{n+1} - S_{n-1}) \quad (2)$$

where the *S* terms are expressed in centimeters of equivalent water height averaged over the entire Congo Basin for the months before and after month *n* (Landerer et al., 2010). The uncertainty of *dS/dt* is calculated as half of the difference between the highest and lowest *dS/dt* values from the three GRACE *S* solutions in any given month (Lee et al., 2011)

Beginning in early 2011, the GRACE mission began an active battery management strategy that resulted in data gaps every several months. In order to reconstruct *dS/dt* data from 2011–2016, we use its average seasonal cycle and~~to~~ correct for ~~interannual~~ variability based on the ~~amount of that variability in nearby~~deviations of adjacent months from their~~at~~ long-term averages. First, the mean monthly cycle of *S* was calculated from data-complete months from 2002–2016. For every missing month from 2011–2016, the average *S* from the two other months in the same season of the same year (DJF, MAM, JJA, and SON) was compared to the corresponding value from the multi-year *S* means. The resulting ratio was then multiplied by the multi-year *S* mean of the missing month to create the reconstructed *S* value. Because the sum of multi-year mean *S* values from October and November is nearly equal to zero and consequently produces unrealistically-scaled values for September, missing September values were instead interpolated using August and October of the same year. Repeating the same procedure for months that are available in the GRACE dataset (i.e. calculating what the reconstructed value would be if it were not available, and comparing it to the observations) shows that this seasonal-scaling interpolation reproduces true *S* fairly accurately: from 2002–2016, each of the twelve months was reconstructed with a mean R^2 of 0.75 and a mean root mean square error (RMSE) of 2.80 cm (relative to average seasonal *S* variations of ~10 cm). Applying this procedure to the mean *S* data from the three monthly GRACE solutions produced the complete *dS/dt* time series that determined the study period for our water balance model (4/2002–11/2016).

Due to the uncertainty of precipitation (*P*) estimates in the Congo (Washington et al., 2013), *P* was estimated using an array of five datasets with different methodologies. These five datasets were chosen because recent validation efforts have shown them to be the most accurate for the Congo Basin (Nicholson et al., 2018, 2019). They include gridded precipitation data from the Global Precipitation Climatology Centre (GPCC) Version 7.0, which uses interpolation with a worldwide network of rain gauges to produce monthly precipitation grids (Schneider et al., 2015). GPCC-compiled gauges within the Congo are extremely sparse after 2000 (Nicholson et al., 2019), and the GPCC ~~version~~ Version 7.0 product only lasts through 2013. The Tropical Rainfall Measuring Mission (TRMM) 3B43 Version 7 product (also known as TRMM Multi-~~Satellite~~ satellite Precipitation Analysis or TMPA), which consists of monthly mean precipitation rate grids, is generated using microwave and infrared sensors on TRMM and other satellites as well as gauge data from the GPCC (Huffman et al., 2007). The Precipitation Estimation from Remotely Sensed Information using Artificial Neural Networks: Climate Data Record (PERSIANN-CDR) product uses satellite infrared data and a neural network approach, calibrated with precipitation forecasts, microwave data, and GPCC gauge data, to produce grids of precipitation estimates at the daily timescale (Ashouri et al., 2015). While PERSIANN is also available without the GPCC gauge corrections that make PERSIANN-CDR so similar to GPCC v7 and TRMM 3B43 over the Congo Basin (Nguyen et al., 2018), it was not used here because it severely overestimates *P* across Africa (Beighley et al., 2011; Thiemig et al., 2012). ~~Recent~~ Several recent studies have found that TRMM Version 7 3B43 and PERSIANN-CDR both perform reasonably well over central Africa (Munzimi et al., 2015; Awange et al., 2016; Camberlin et al., 2019).

Notably, the above three products all depend on GPCC rain gauges to some degree. As a result, all three datasets feature similar rainfall trends and model performance over the Congo Basin during the 2002–2016 period studied here and cannot be considered truly independent *P* datasets (Nicholson et al., 2019). To that end, the Climate Hazards Group Infrared Precipitation with Stations Version 2.0 (CHIRPS2) product, which uses two thermal infrared datasets and interpolated gauge data, was also included as a more independent dataset (Funk et al., 2015). The CHIRPS2 product was recently found to be among the most accurate rainfall datasets on monthly timescales within the Congo Basin (Camberlin et al., 2019).While CHIRPS2 does incorporate some gauge data that overlap with the GPCC product, it is not scaled to fit GPCC data to the same extent as TRMM 3B43 or PERSIANN-CDR are over central Africa (Nicholson et al., 2019)—in fact, the near-total lack of rain gauges within the basin in both CHIRPS2 and GPCC leads to a low correlation between the two datasets within the study area (Funk et al., 2015), indicating the *P* datasets maintain a high degree of independence. Finally, a recent gauge-based dataset developed for the Congo Basin, NIC131-gridded, served as another independent precipitation data source with coverage through 2014 (Nicholson et al., 2018). The monthly 2.5° NIC131-gridded product was created by applying a spatial reconstruction technique based on principal component analysis to a gauge network that, due to the severe decline of GPCC coverage during the 1990s, is largely independent of the GPCC's gauges in Africa (Nicholson et al., 2019).

2.2 Comparing and ~~unifying~~ merging precipitation estimates

Because the above five datasets each individually remain highly uncertain, and because no accurate independent basin-wide validation is possible, triple collocation (TC) was used to estimate the error statistics of the different datasets, and ultimately combine them by weighting them according to their relative errors. TC is a method for characterizing systematic and random errors in geophysical measurements using three independent, collocated time series, ~~and~~ even if these datasets are individually noisy (Stoffelen, 1998; McColl et al., 2014). It is particularly valuable in gauge-sparse regions like the Congo Basin because it does not rely on independent error-free validation data. TC-based error calculations have previously been used in a wide variety of geophysical settings—among others, TC was recently used to determine the relative weightings of different hydrologic flux estimates in a neural network-based data combination effort in a manner conceptually analogous to its use here (Alemohammad et al., 2017), and other work has confirmed the ability of TC to merge *P* datasets into a single more accurate dataset (Dong et al., 2020). Rather than the linear model used in most TC applications, we used a multiplicative model that is more appropriate for quantifying errors in precipitation estimates (Alemohammad et al., 2015). In the multiplicative error model, true precipitation rate T is assumed to be related to the estimated precipitation of product i, P_i, as follows:

$$P_i = a_i T^{\beta_i} e^{\epsilon_i} \quad (3)$$

in which a_i is the multiplicative error, β_i is the deformation error, and ϵ_i is the random residual error (which is assumed to have a mean of zero).

Assuming the three collocated precipitation estimates' residual errors are uncorrelated with each other, and are uncorrelated with the true precipitation values, the RMSEs of all three input *P* datasets may be calculated with Eqs. (4–6):

$$\sigma_{p_1}^2 = C_{11} - \frac{C_{12}C_{13}}{C_{23}} \quad (4)$$

$$\sigma_{p_2}^2 = C_{22} - \frac{C_{12}C_{23}}{C_{13}} \quad (5)$$

$$\sigma_{p_3}^2 = C_{33} - \frac{C_{13}C_{23}}{C_{12}} \quad (6)$$

where $C_{i\,j}$ is the (i, j)th element of the sample covariance matrix between the three log-transformed datasets and σ_{pi} is the RMSE of the log-transformed P_i time series. σ_{pi} can be converted to the actual RMSE of P_i by multiplying by the mean value of P_i (Alemohammad et al., 2015).

The errors of the five *P* datasets were evaluated by applying TC to triplets of products deemed relatively independent. That is, TC was repeated three times using different triplets: TRMM–NIC131–CHIRPS2, GPCC–NIC131–CHIRPS2, and PERSIANN–NIC131–CHIRPS2. The three RMSEs calculated for NIC131-gridded and CHIRPS2 were then averaged and compared to the RMSEs calculated for TRMM, GPCC, and PERSIANN-CDR. In order to combine the most accurate *P* time series (and their estimated errors) into a single unified *P* estimate, weighting factors were assigned to each time series in a manner inversely proportional to the product RMSE. That is, each weighting factor w_i was assigned as in (Eq. 7):

$$w_i = \frac{RMSE_i^{-1}}{\sum_1^3 RMSE_i^{-1}} \quad (7)$$

The best-estimate rate of precipitation for each month was then calculated as a weighted average across ~~all five original~~the three independent precipitation products~~,~~ using w_i. The resulting dataset's RMSE was also used to propagate precipitation uncertainty into the uncertainty of ET_{wb} using a root-mean-square sum of the weighted errors. While longer time series are generally preferred for ~~use in~~ TC in order to reduce sampling error, data prior to 2002 were discarded in the TC analysis because the greater number of rain gauges ~~prior to 2002~~ likely leads to different error statistics than in this period (Nicholson et al., 2018).

2.3 Comparison to global ET products

Many hydrological studies of the Congo Basin rely on global ET products to constrain their models (e.g. Hassan and Jin, 2016; Ndehedehe et al. 2018~~; Hassan and Jin 2016~~). We analyzed ~~six~~ seven widely-used global ET data products and evaluated their performance relative to ET_{wb}. MOD16A2 Version ~~5~~ 6 is a global ET data product based on the Penman-Monteith equation, meteorological reanalysis, and remotely-sensed land surface data from the Moderate Resolution Imaging Spectroradiometer (MODIS) satellite mission (Mu et al., 2013). The Operational Simplified Surface Energy Balance (SSEBop) Version 4 model uses remotely-sensed thermal data from MODIS and global weather datasets to produce gridded ET estimates at a very high (1 km) spatial resolution (Senay et al., 2013). The Global Land Evaporation: Amsterdam Model Version 3.~~1a~~3a (GLEAM v3.~~1a~~3a) product estimates Priestley-Taylor potential ET (PET) from reanalysis radiation and temperature data, then reduces PET to actual ET using remotely sensed soil moisture and vegetation optical depth measurements (Miralles et al., 2011; Martens et al., 2017). Modern-Era Retrospective Analysis for Research and Applications, Version 2 (MERRA~~-~~2) is a reanalysis product that integrates a wide variety of observation types from satellites and in-situ sources to produce terrestrial ET estimates using a water balance approach (Gelaro et al., 2017). The Global Land Data Assimilation System Version 2.1 Noah (GLDAS-Noah) product is a land surface simulation forced by a combination of model and observation datasets that provides monthly mean ET estimates (Rodell et al., 2004b).

Lastly, two global ET products based on upscaling tower data from the global FLUXNET eddy covariance network (Baldocchi et al., 2002) were included: the Model Tree Ensemble (FLUXNET-MTE) product uses a tree-based machine learning approach to upscale carbon, water, and energy flux observations using external global data sources, resulting in a monthly 0.5° global dataset (Jung et al., 2011). The more recent FLUXCOM product uses machine learning algorithms and additional time-varying meteorological inputs to achieve greater accuracy in upscaling eddy covariance~~flux~~ tower data (Jung et al., 2019). This study uses FLUXCOM's daily RS+METEO version because of its lower ET uncertainty in Africa (Jung et al., 2019). However, it should be noted that FLUXNET-MTE and FLUXCOM, like the physical modeling approaches above, have primarily been validated against observational data in the mid-latitudes. There are no FLUXNET towers located within the Congo ~~basin~~ Basin that could have been used for training these and other models~~. All datasets were averaged across the Congo basin using linear interpolation.~~.

The accuracies of these ~~six~~ seven products were evaluated by comparing them to the monthly ET_{wb} values: RMSEs, Pearson correlation coefficients, and Taylor skill scores were calculated for each dataset versus ET_{wb}. Only the years

~~2002~~2003–2011 are common to all ~~six~~ seven ET datasets and the GRACE *S* data, so all statistics were calculated over this period. Pearson correlation coefficients help determine the ability of each ET model to predict ET_{wb}, while Taylor skill scores allow a comparison of the variability present in each model by accounting for their standard deviations (Taylor, 2001). The average seasonal cycles and interannual variations of the products are also compared to better understand similarities and differences between the products.

2.4 Meteorological and vegetation data

To examine potential drivers of ET's seasonality, interannual variability, and long-term trends in the Congo Basin, ET_{wb} is compared to a host of meteorological and vegetation data including photosynthetically-active radiation (PAR), net radiation (R_n), vapor-pressure deficit (VPD), air and skin temperatures (T_a and T_s), solar-induced fluorescence (SIF), and enhanced vegetation index (EVI). We used all-sky monthly mean PAR and R_n data from the Clouds and the Earth's Radiant Energy System (CERES) project's 1° gridded products. PAR data were derived from the synoptic surface flux model (SYN1deg) (Doelling, 2017), which divides surface PAR fluxes into direct (PAR_{dir}) and diffuse (PAR_{diff}) components, while R_n data were derived from the Energy Balanced and Filled (EBAF) climate data record (Loeb, 2017). The global reanalysis model ERA-Interim (Dee et al., 2011) provided surface air temperature and relative humidity data in 6-hour increments, which were used to calculate monthly VPD means of the entire basin using linear interpolation. Although reanalysis models over Central Africa remain uncertain and poorly constrained (Lorenz and Kunstmann, 2012; Brands et al., 2013), these VPD values were tested against hourly VPD data from Automated Surface Observing Systems (ASOS) and Met Office Integrated Data Archive System (MIDAS) weather reports from the Congo Basin (Met Office, 2012) and were found to capture monthly cycles of VPD with acceptable accuracy (Fig. S1).

Monthly mean T_a and T_s from the Congo Basin were sourced from the ascending (daytime) retrievals of the Atmospheric Infrared Sounder (AIRS) Level 3 monthly product (Kahn et al., 2014). The 740 nm SIF data from the Global Ozone Monitoring Experiment 2 (GOME-2) platform were retrieved from the GOME2_Fluorescence Version 26 Level 3 dataset (Joiner et al., 2013). The GOME-2 SIF dataset is known to have suffered from a significant sensor decay problem resulting in a spurious worldwide downward trend~~, so the SIF data were not used in any long-term trend analyses~~ (Zhang et al., 2018), so the SIF data were not used in any long-term trend analyses. SIF was normalized by monthly CERES total PAR data in order to isolate the effects of phenological, physiological, and hydrological variability on plant productivity independent of radiative controls (Madani et al., 2017; Pagán et al., 2019). MODIS Collection 6 EVI data processed with the Multi-Angle Implementation of Atmospheric Correction (MAIAC) algorithm were converted to monthly means from 8-day composite rasters (~~Huete et al., 2002;~~ Lyapustin et al., 2018). The MAIAC algorithm, which eliminates errors from aerosols and sun-sensor geometry issues in MODIS data, has previously proven beneficial for examining vegetation greenness in tropical forests (~~Hilker et al., 2012;~~ Lyapustin et al., 2011a~~; Lyapustin et al.~~, 2011b~~; Lyapustin et al.~~, 2012; Hilker et al., 2012; Bi et al., 2016). Lastly, annual land cover data from the MODIS-based MCD12C1 Version 6 dataset were retrieved for 2002–2016 and modally-averaged to produce a single land cover classification of the Congo Basin (Friedl and Sulla-Menashe, 2015). Pixels

were aggregated into dominantly deciduous or evergreen vegetation types according to the International Geosphere-Biosphere Programme's (IGBP) 17-class land cover scheme, with savannas and grasslands considered deciduous and permanent wetlands considered evergreen. Other vegetation types that are more difficult to generalize (e.g. croplands, mixed forests, and shrublands) were spatially-limited enough to be ignored once the land cover data were majority-resampled to match the 1° pixel size of our study's coarsest datasets (Fig. S2).

2.5 Removing seasonal cycles and long-term trends

In order to track interannual correlations between ET_{wb}, meteorological variables, and vegetation indices, the Breaks for Additive Season and Trend (BFAST) R package (Verbesselt et al., 2015) was used to search for abrupt changes in the trends of our time series, identify linear long-term trends, and remove ~~the~~ average seasonal cycles from the data (Verbesselt et al., 2010a, 2010b).

3 Results

3.1 Triple collocation of precipitation datasets

The results of the TC analysis are provided in Table 1. NIC131-gridded exhibited the lowest RMSE in all three triplets, from 0.60 cm/month to 0.72 cm/month (mean 0.65 cm/month) depending on the triplet. The TC results indicate that NIC131-gridded, a Congo-specific gauge-based dataset designed using meteorological stations absent from the GPCC network and a principal component-based statistical approach, is the best currently-available *P* dataset for the Congo Basin after 2002 (Nicholson et al., 2018). The results in Table 1 agree well with those of Nicholson et al. (2019), which found CHIRPS2 and PERSIANN-CDR to be more accurate than TRMM and GPCC in the Congo Basin after 1998. Prior work has also demonstrated that CHIRPS2 is among the best *P* products available for central Africa and outperforms TRMM and PERSIANN-CDR on a monthly basis (Dembélé and Zwart, 2016; Camberlin et al., 2019; Nicholson et al., 2019), consistent with the results in Table 1. Given the decreasing availability of Congolese rain gauge data in the GPCC database and the difficulty of measuring *P* with ~~satellites~~ satellite remote sensing in central Africa (McCollum et al., 2000; Yin and Gruber, 2010; Awange et al., 2016; Nicholson et al., 2018), it is not surprising that the GPCC-based products generally displayed higher errors.

Table 1: Root mean square errors (RMSEs) for the five P datasets (in three triplets) evaluated in this study, as well as the weighting factors used to unify the three most accurate datasets. All values are presented ~~in~~ in units of cm/month.

Dataset	RMSE Triplet 1	RMSE Triplet 2	RMSE Triplet 3	Mean RMSE	Weighting Factor
TRMM 3B43	1.67	-	-	1.67	-
GPCC Version 7	-	1.66	-	1.66	-
PERSIANN-CDR	-	-	1.60	1.60	0.19

NIC131-gridded	0.65	0.72	0.60	0.65	0.47
CHIRPS2	0.93	0.88	0.96	0.93	0.33

TRMM, GPCC, and PERSIANN-CDR—which all integrate GPCC rain gauges in some capacity—are highly correlated and therefore feature similar RMSEs between 1.60 cm/month (PERSIANN-CDR) and 1.67 cm/month (TRMM). Therefore, our subsequent analyses discard GPCC and TRMM and use only PERSIANN-CDR—, the most accurate of the three GPCC gauge-related datasets. As discussed in Sect. 2.2, PERSIANN-CDR was implemented in a weighted average in combination with NIC131-gridded and CHRIPS2 to create a unified *P* time series, P_{TC}. The NIC131-gridded dataset only lasts through 2014, so from 2015–2016 only CHIRPS2 and PERSIANN-CDR were used in P_{TC}. The uncertainty in P_{TC} was estimated to be 0.30 cm/month from 2002–2014 and 0.59 cm/month from 2015-2016 (after NIC131-gridded data coverage ends)—both lower than the RMSEs of any of the individual *P* products tested.

3.2 Water balance ET estimates

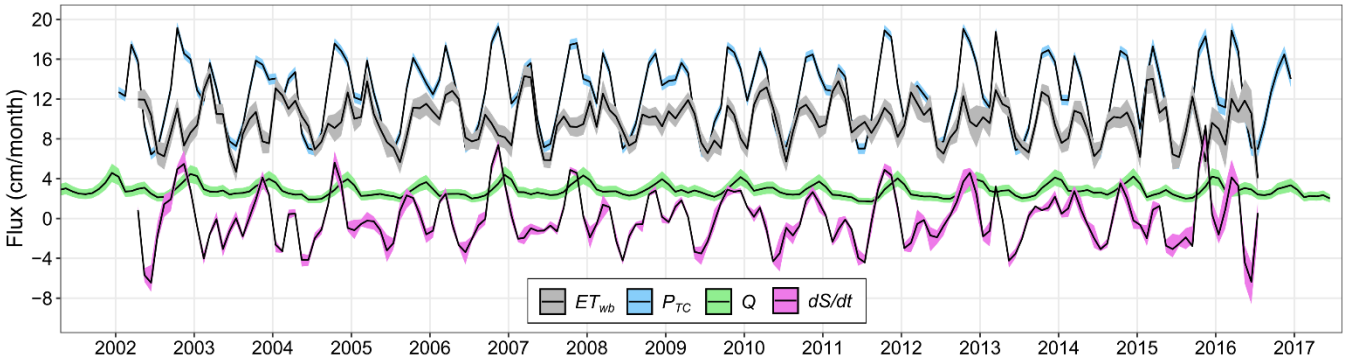

In Fig. 1, clear seasonal cycles as well as interannual variations are visible in all four of the hydrologic fluxes from Eq. 1: the rainy MAM and SON seasons show local peaks in ET_{wb} as well as *dS/dt*, which is generally a negative flux (representing water leaving the land surface system) for most of the rest of the year. *Q* has the least temporal variability of the fluxes and is the smallest in magnitude, although it exhibits increased runoff 1–2 months after the primary SON rainy season. Mean annual ET_{wb} is 117.2±3.5 cm/year (calculated from 2003–2015, the data-complete years of the study period). Mean annual P_{TC} from 2003–2015 is 150.4±2.6 cm/year, and mean annual *Q* is 33.7 cm/year. ~~The~~ *dS/dt*, which fluctuates between positive and negative values, ranges from −3.2 to 3.7 cm/month on average.

Figure 1: Time series of the four water balance components from 2002-2016. Data are monthly, basin-wide averages in cm water height equivalents. Black lines represent mean values; ribbons represent uncertainty ranges.

Plotting monthly means of the water balance fluxes provides further clarity regarding their seasonal cycles (Fig. 2). The basin-wide seasonal flux cycles are dominated by contributions from the region south of the equator, which comprises the majority of the Congo Basin (Fig. S2). October and November are the rainiest months, followed by March and April, while

June and July are the driest months of the year. ~~The~~ Positive *dS/dt* rates indicate *S* regenerates mostly during the very wet October and November months and less so during December, the secondary rainy season in March and April, and in September with the onset of the primary rainy season. *S* loses water fastest during May and June, reaching its minimum during June, when ET_{wb} exceeds P_{TC} on average (Matsuyama et al., 1994). Interestingly, while ET_{wb} tracks the seasonality of P_{TC} to an extent, it peaks in March during the secondary rainy season rather than during the primary, wetter, SON wet season. The possible causes of this difference between precipitation and ET seasonality are analyzed further in Sect. 4.2.

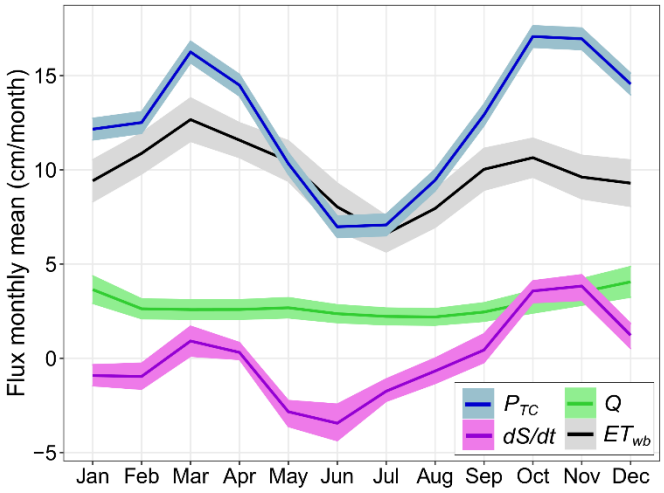

Figure 2: Mean monthly cycle of the four water balance components from 2002-2016. Dark lines represent mean values; ribbons represent uncertainties.

Table 2 summarizes fourteen mean annual ET estimates from the Congo Basin found in the literature. The studies produce a mean ET of 116.8~~7~~ cm/year with a standard deviation of 6.6~~8~~ cm/year and a median ET of 118.9~~6~~ cm/year, although different study periods and a variety of methods were used to estimate actual ET. All but one historical ET estimate fall within 10% of mean annual ET_{wb}, showing good agreement between the present study's ET estimates and prior literature on the subject.

Table 2: Historical estimates of mean annual basin-wide ET from the literature. Mean and median values are derived from the literature and presented alongside the mean annual ET_{wb} from this study.

Source	Mean ET (cm/yr)	Time span
Balek 1977	124.8	climatology
Balek 1983	122.4	climatology
Bricquet 1988	123.0	climatology
Bultot 1971	119.6	climatology
Chishugi and Alemaw 2009	109.8	1961–1990
Matsuyama et al. 1994	125.0	1985–1988

Nicholson et al. 1997	112.7	climatology
Oki et al. 1993	120	1985–1988
Olivry et al. 1993	108.6	1951–1990
Pan et al. 2012	~102	1984–2006
Pinet and Souriau 1988	118.2	climatology
Russell and Miller 1990	114	climatology
Shem 2006	122.3	1979–1994
Ukkola and Prentice 2013	~111	1963–1998
Weerasinghe et al. 2020	118.6	1979–2010
Mean:	116.~~7~~8	
Median:	118.~~9~~6	
This study	117.2±3.5	2003–2015

3.3 Comparing the ET_{wb} seasonal cycle to global ET models

The seasonal cycle of ET_{wb} is compared to those of ~~six~~ seven global ET products in Fig. 3. ~~Multiple datasets generally disagree with the magnitude of basin-wide ET_{wb}. Indeed, MOD16A2 and GLEAM v3.1a fall outside the uncertainty range of ET_{wb} more often than not. GLDAS-Noah and FLUXCOM monthly means both fall within the uncertainty range of ET_{wb} eight months out of the year, while MERRA2 does so seven months out of the year.~~ All seven products generally follow the seasonal shape of ET_{wb}, however none capture the full amplitude of ET fluctuations across seasons. Peak basin-wide ET during March is underestimated in all models to some degree, ~~W~~ and ~~hile~~ all seven ~~models display~~overestimate the basin's low JJA ET ~~to some degree, they generally~~while also failing to capture the fast recovery of ET_{wb} from August~~–~~ to September. The period from November to January displays the most consistent departure of global ET products from ET_{wb}, with all seven products overestimating ET during these three months. Most models ~~also~~ do correctly find ET to peak during the MAM rainy season (Matsuyama et al., 1994; Pan et al., 2012; Crowhurst et al., 2020), ~~but all global ET products~~yet they generally underestimate how much larger the MAM ET_{wb} peak is than the SON one. For instance, FLUXNET-MTE plots SON ET as roughly equivalent to MAM ET. ~~The peak ET months for each rainy season also lag those of ET_{wb} for several products.~~ In general, the global ET products ~~fail to capture~~underestimate the magnitude of seasonal variations in ET_{wb}, although some track ET_{wb} much more closely than others.

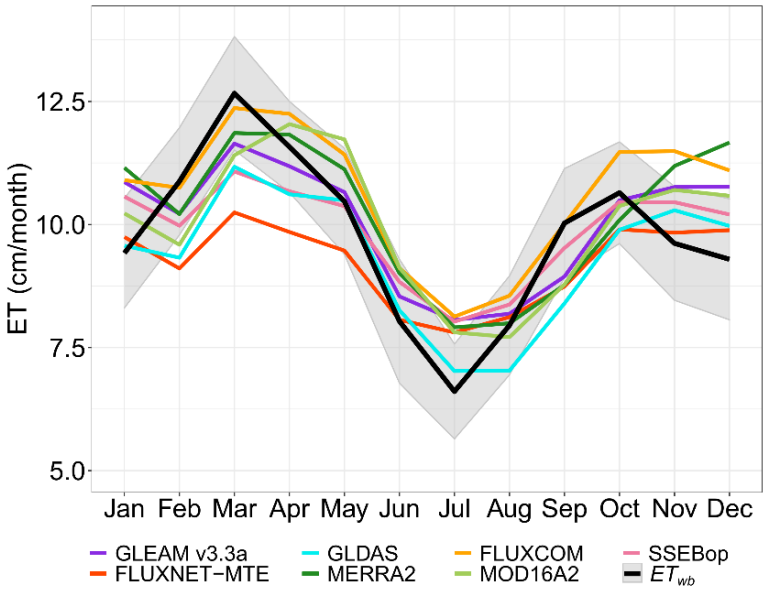

Figure 3: Mean monthly cycle of ET_{wb} plotted alongside the mean monthly cycles of ~~six~~ seven global ET products. The grey ribbon represents ET_{wb} uncertainty.

Global ET products are evaluated against ET_{wb} from 2003–2011 using several metrics in Table 3. Mean annual ET ranges from ~~88~~110.7 cm/year (~~GLEAM v3.1a~~GLDAS-Noah) to 127.6 cm/year (FLUXCOM), compared to the ET_{wb} annual mean of 118.0±3.5 cm/year for that time period. ~~Excepting GLEAM v3.1a and MOD16A2, the global~~ Global ET product annual averages all fall within 10% of ET_{wb}'s, yet no product comes close to the 6.1 cm average difference observed between maximum and minimum ET_{wb}, nor do they match the 2.1 cm standard deviation of the ET_{wb} time series. All models find mean ET during MAM to exceed mean ET during SON, but the global products feature more uniform ET rates within each season (Fig. 3). ~~,~~FLUXCOM produces the highest Pearson correlation coefficient ~~versus~~ with ET_{wb} while MERRA2 produces the lowest; ~~, and~~ FLUXCOM, GLDAS-Noah, and MERRA2 ~~again leads all~~ lead the products in Taylor skill score while FLUXNET-~~-~~MTE ~~demonstrates~~ achieves the lowest score. ~~FLUXCOM~~ GLEAM v3.3a ~~also~~ features the lowest RMSE relative to ET_{wb}; ~~GLEAM v3.1a~~ while MERRA2 features the highest. FLUXNET-MTE and SSEBop both exhibit very low standard deviations that manifest in low Taylor scores, suggesting these products are the worst at representing variability in Congo Basin ET. ~~GLEAM v3.1a underestimates mean annual ET_{wb} by nearly 25%, exhibits a low Taylor score, and has the highest RMSE of all six products. MOD16A2 has the second-highest RMSE of the six products evaluated and generally underestimates the magnitude and seasonality of ET_{wb} in the Congo Basin while achieving a correlation coefficient of only 0.54 and a Taylor score of 0.58.~~

Table 3: Mean annual ETs, mean seasonal amplitudes, ratios of seasonal mean ET from MAM over SON, ~~from 2003-2011 alongside~~ Pearson correlation coefficients, Taylor skill scores, RMSEs, and standard deviations from ~~2002~~2003-2011 for ~~six~~ seven global ET products in comparison to ET_{wb}.

ET product	Mean annual ET (cm)	MAM amplitude (cm)	JJA amplitude (cm)	ET_{MAM}/ET_{SON}	Pearson correlation coefficient	Taylor skill score	RMSE (cm)	Standard deviation (cm)
ET_{wb}	118.0±3.5	2.9	−3.2	1.15	-	-	-	2.1
MOD16A2	~~94.2~~120.1	2.0	−2.3	1.18	0.~~54~~59	0.~~58~~70	~~2.7~~1.7	1.~~3~~4
SSEBop	117.9	1.2	−1.9	1.06	0.68	0.48	1.6	0.9
GLEAM	~~88.7~~120.3	1.6	−2.0	1.11	0.~~53~~68	0.~~40~~64	~~3.0~~1.5	~~0.9~~1.2
FLUXNET-MTE	111.1	1.0	−1.4	1.04	0.~~63~~64	0.~~36~~39	1.8	0.8
FLUXCOM	127.6	1.7	−2.5	1.09	0.~~74~~73	0.~~71~~72	1.6	1.~~3~~4
GLDAS-Noah	110.7	1.8	−2.3	1.13	0.~~64~~70	0.~~69~~72	1.~~7~~6	1.4
MERRA2	119.7	1.6	−2.2	1.16	0.~~43~~47	0.~~68~~72	2.~~1~~0	1.~~7~~8

3.4 Drivers of ET seasonality and variability

As discussed in Sect. 3.2, the shape of ET_{wb}'s seasonal cycle roughly follows that of P_{TC}, since water availability and vegetation productivity modulate ET. However, ET_{wb} is greater during the MAM rainy season than in the SON rainy season, despite the latter season being wetter than the former. On average, ET_{wb} also exceeds P_{TC} during June. These findings are consistent with previous studies that found basin-wide ET can peak during MAM (Matsuyama et al., 1994; Pan et al., 2012; Crowhurst et al., 2020), although the drivers behind this seasonal cycle are less clear. To help develop hypotheses on the nature of ET's drivers, monthly mean ET_{wb} is compared here to several climatic drivers and indices reflecting ~~seasonally~~ seasonally-varying vegetation activity (Fig. 4).

Possible environmental drivers of ~~the~~ ET_{wb}'s seasonality include soil water availability, water demand from VPD, solar ~~radiation~~irradiance, and temperature. GRACE-derived S can be assumed to be a partial proxy for water availability (though note that not all water measured by S is necessarily accessible to plant roots or available for soil evaporation; see Sect. 4.2.4). S is significantly lower during SON than MAM when considering the entire basin (Fig. 4f), consistent with the relatively lower SON ET_{wb}. The relatively lower SON S could be due to the much lower precipitation during JJA than DJF (Fig. 3) and/or due to a seasonal difference in how much of the rainfall infiltrates the land surface. VPD is fairly low in both wet seasons,

although still elevated in September following the JJA dry season (Fig. 4e). R_n is lower during the SON wet season than the MAM, likely contributing to the lower ET_{wb} in SON (Fig. 4c).

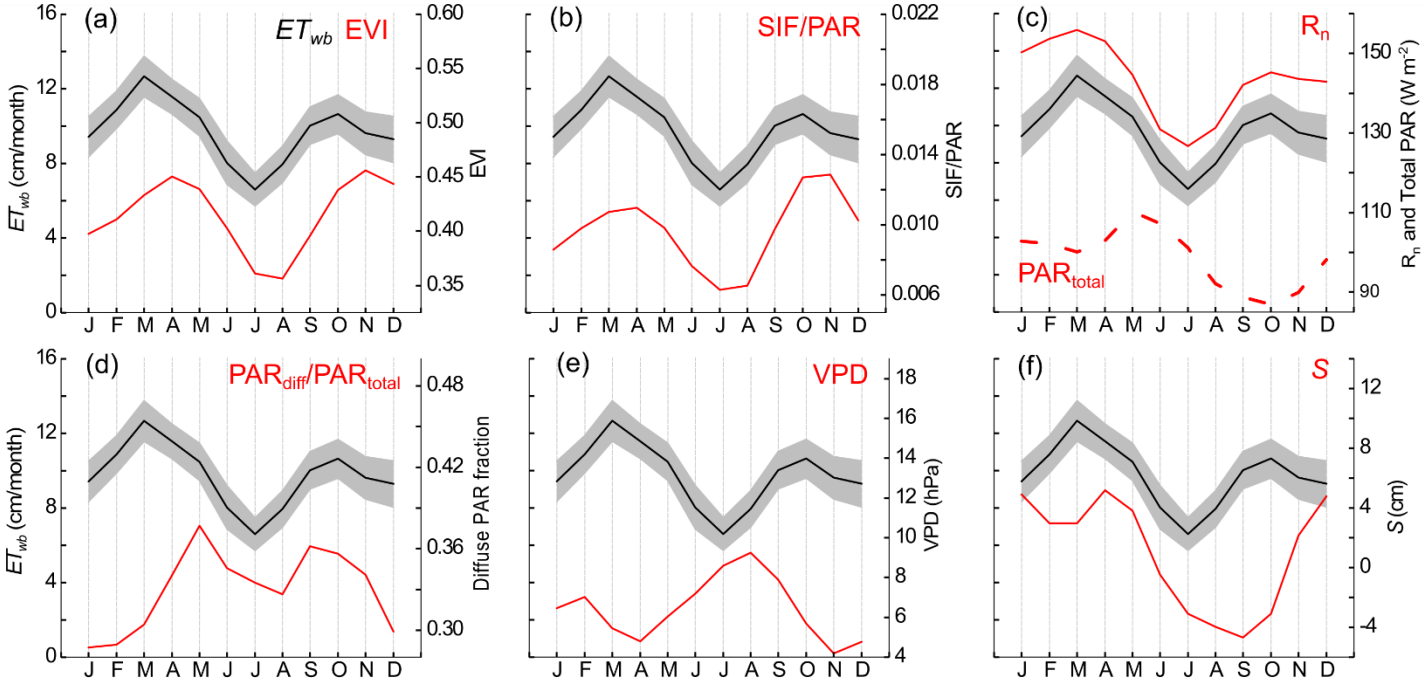

Figure 4: Mean monthly cycle of ET_{wb} (black line with gray uncertainty range) plotted alongside those of (a) MAIAC-processed EVI, (b) SIF/PAR, (c) R_n and total PAR, (d) Diffuse PAR fraction (PAR_{diff}/PAR_{total}), (e) VPD, and (f) S from GRACE (red lines). Data are averaged over the entire basin area. Note that the mean ET_{wb} curve and scale is the same in each sub-panel.

The variability of ET is expected to be linked to vegetation phenology through the large contribution of transpiration to overall ET in the densely vegetated Congo Basin (Lian et al., 2018). However, both MAIAC EVI (Fig. 4a) and PAR-normalized SIF (Fig. 4b) show greater vegetation greenness and photosynthesis, respectively, during the SON wet season than during the MAM wet season (SIF peaks in October and November with or without PAR normalization, indicating both greater total photosynthesis and more light-efficient production during these months; see Fig. S3). ~~This~~ The high SON productivity without correspondingly high ET_{wb} suggests relatively greater water use efficiency (WUE, or the ratio of photosynthetic production to the amount of water transpired through plants' stomata) in SON and/or a relatively greater contribution of direct soil/canopy evaporation to ET in MAM (although bare soil evaporation is expected to be a minority of total ET in the densely-forested basin; see Sect. 4.2). ~~This greater water use efficiency~~WUE during ~~the~~ SON ~~than the~~may be higher than in ~~MAM~~ March and April (when ET_{wb} peaks) ~~season could also be driven by~~because of ~~a~~the ~~relatively~~ greater ratio of diffuse PAR to total PAR during SON (Fig. 4d) which can increase photosynthetic efficiency (Mercado et al., 2009), as further discussed in Sect. 4.2.3.

The basin-wide analyses in Fig. 4 are almost certainly masking significant sub-basin variability. The sub-basin division of ET is not known, and dividing the coarse-resolution *S* at the sub-basin level is also highly uncertain. Nevertheless, we considered the sub-basin variation of ~~select productivity and climatic metrics~~MAIAC EVI, PAR-normalized SIF, and VPD in ~~(~~Fig. 5~~)~~. The basin was divided into the equatorial evergreen forest ~~(which straddles the equator)~~region, ~~Northern~~ northern deciduous ecosystems, and ~~Southern~~ southern deciduous ecosystems (Fig. S2). The deciduous regions feature larger seasonal variations in all three variables than the evergreen forest does ~~(Fig. 5)~~, but the opposite seasonalities of the ~~Northern~~ northern and ~~Southern~~ southern regions partially offset one another and produce basin-wide EVI and SIF/PAR cycles that are ~~broadly~~ roughly similar to those of the evergreen forest (Figs. 4a, b; 5b). The greater extent of the Southern deciduous region results in basin-wide EVI and SIF/PAR minima during JJA rather than DJF, and basin-averaged VPD likewise peaks during JJA (Fig. ~~5e~~4e) despite its low variability in the extensive evergreen forest region (Fig. 5b). Taken together, the results of Fig. 5 suggest that a basin-wide analysis is informative despite averaging over multiple vegetation types.

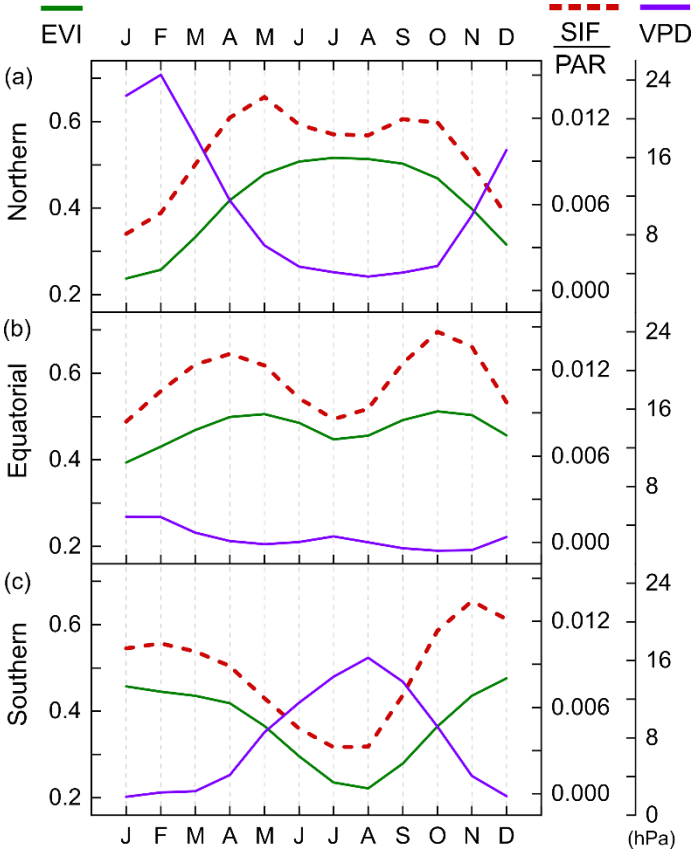

Figure 5: (a) Average monthly cycles of MAIAC-processed EVI (green line), SIF/PAR (red dashed line), and VPD (purple line) for the northern deciduous area of the Congo Basin. (b)-(c) As with (a), but for the equatorial evergreen and southern deciduous regions, respectively. Scales are consistent between plots (a)-(c) for each variable.

3.5 Long-term climatic shifts and their impacts in the Congo Basin

We detect no significant linear trends in ET_{wb}, P_{TC}, dS/dt, or Q from 2002–2016 after removing average seasonal cycles with BFAST (Fig. 6). However, several interannual trends are detectable in other environmental data (Fig. 7~~).~~): PAR, R_n, and VPD all increase significantly from 2002–2016 after the average seasonal cycle is removed from the time series, indicating the Congo Basin has become sunnier and less humid in recent years. This progression to sunnier and less humid conditions in the Congo Basin is not reflected in ET_{wb} and productivity (as measured by MAIAC EVI), which do not show long-term changes over the past two decades (Figs. 6d, 7d).

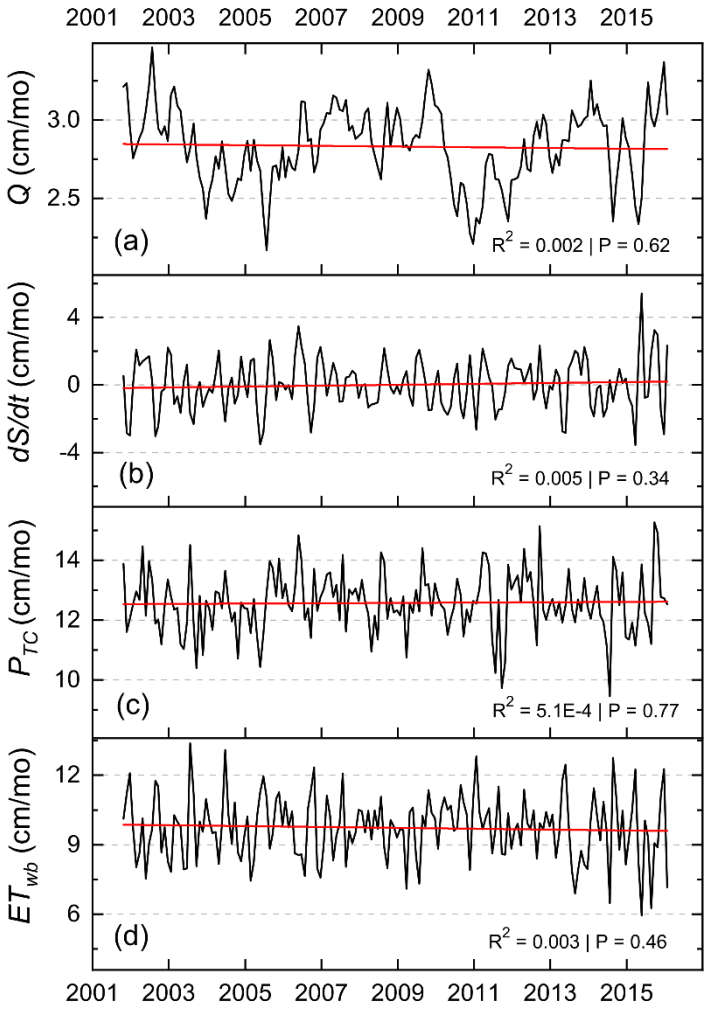

Figure 6: Linear regressions of deseasonalized monthly (a) *Q*, (b) *dS/dt*, (c) P_{TC}, and (d) ET_{wb}.

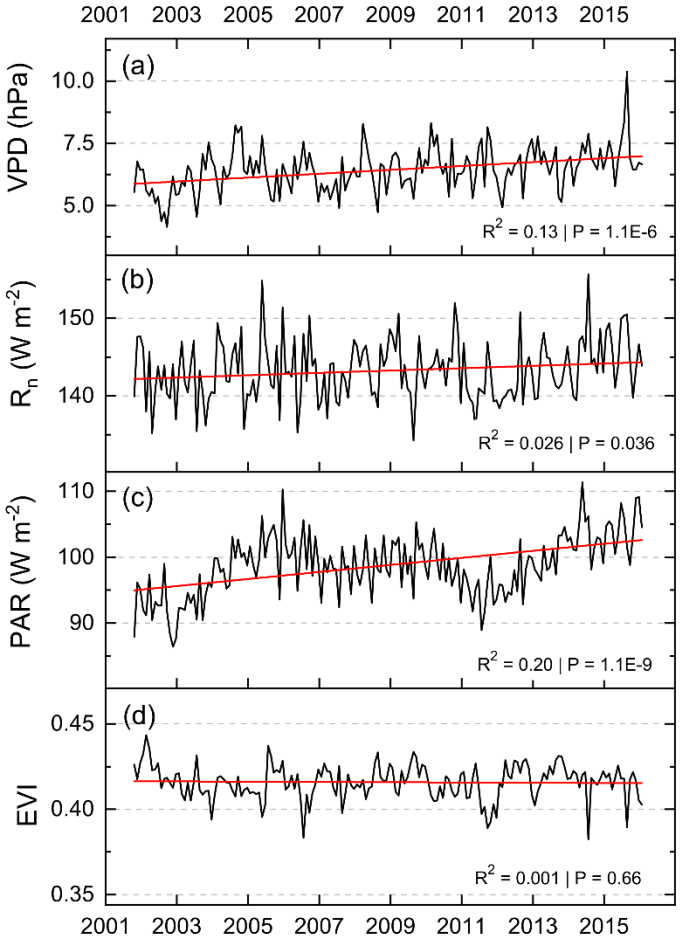

Figure 7: Linear regressions of deseasonalized monthly (a) VPD, (b) R_n, (c) PAR_{total}, and (d) MAIAC EVI.

4 Discussion

4.1 The value of water balance-based ET estimates~~estimation in the Congo Basin~~

The scarcity of operational precipitation gauges and complete lack of eddy covariance towers within the Congo river basin have previously restricted ET estimates to process-based models, short-term ET observations at site scale, and global products with insufficient validation in tropical Africa. The water balance-based ET_{wb} derived here provides a basin-wide constraint on ET. It has an uncertainty that is relatively low compared to its average seasonal cycle (Fig. 2), and its magnitude matches well with previous long-term ET estimates from the basin (Table 2). The shape of its annual seasonal cycle (with ET_{wb} peaking in MAM rather than in SON) also agrees with several previous ET modeling efforts in the basin (Matsuyama et al., 1994; Pan et al., 2012; Crowhurst et al., 2020). These findings support the accuracy of the water balance model in estimating basin-wide

ET~~, and indicate the combination of *P* products used is relatively accurate when considered across the basin and aggregated using triple collocation.~~.

The results of this study also reinforce the value of the inverted water balance method for studying river basins large enough to accommodate the coarse spatial resolution of GRACE data. Compared to the difficulty of directly measuring ET and the large amount of observational data needed to constrain ET models, the inverted water balance is conceptually straightforward and has relatively simple data requirements. But as demonstrated here and in other large river basins like the Amazon (Maeda et al., 2017; Swann and Koven, 2017), inverting the water balance produces robust estimates of ET which can be used to validate and improve other ET models' representation of sparsely-observed basins. Limitations of water balance ET estimates include the coarse spatial resolution, monthly timesteps, and short temporal coverage of GRACE (2002–2016, with various data gaps), the availability of river discharge data for the area of interest, and the quality of gridded *P* data in the region. However, the use of *dS/dt* data may not be necessary in long-term ET estimates (Weerasinghe et al. 2020), so the limitations of GRACE data mostly affect studies examining ET variability on annual or shorter timescales. The uncertainties of *P* datasets can be assessed and mitigated using techniques such as TC (Stoffelen 1998; McColl et al., 2014; Alemohammad et al. 2015; Dong et al. 2020), but basins with more thorough gauge coverage than the Congo probably do not require such thorough analysis of multiple gridded *P* products.

4.2 The seasonal imbalance of ET_{wb} and *P* maxima

As expected, the seasonal cycle of ET_{wb} mostly follows that of precipitation, with two annual dry and two annual wet seasons. However, the seasonal cycles of *P* and ET_{wb} feature an interesting offset: whereas SON is the wetter of the two rainy seasons, ET_{wb} is greater during MAM than during SON (Fig. 2). The ET_{wb} peak during MAM is supported by several previous modeling efforts with a variety of methodologies (Matsuyama et al., 1994; Pan et al., 2012; Crowhurst et al., 2020), indicating it is not simply an artifact of the water balance model or the data sources used here. Yet the underlying causes of the imbalance are not well understood (Crowhurst et al., 2020). We evaluated several possible drivers of the observed MAM peak in ET_{wb} including phenology, photosynthetic production (via EVI and SIF), terrestrial water availability (via GRACE-derived *S*), PAR, R_n, VPD, T_a, and T_s. Ultimately, we conclude that ~~the availability of radiative energy~~higher levels of solar irradiance (especially photosynthetically-favorable diffuse radiation) and greater soil water availability during MAM provide~~s~~ the most likely explanation for ~~its~~ seasonally high ET rates.

As transpiration is the dominant component of ET throughout the Congo Basin (Lian et al., 2018), primary productivity (through its links to stomatal closure and active leaf area) likely explains the seasonality of ET_{wb} to some degree. In fact, recent studies have found that evergreen forests in ~~equatorial Africa~~an equatorial section of the Congo exhibit a similar greenness seasonality to the seasonality of ET_{wb}, with a bimodal cycle generally aligning with *P* but peaking in MAM instead of the wetter SON (Betbeder et al., 2014; Philippon et al., 2016). However, these studies focused on specific areas of evergreen forests and wetlands that may not represent the ecohydrology of the Congo Basin's entire equatorial rainforest belt, and used MODIS products that ~~did~~ do not fully account for sun-sensor geometry and other sources of error at low latitudes (Hilker et

al., 2012; Bi et al., 2016). To this end, the MAIAC algorithm (Lyapustin et al., 2018) reduces noise and increases the availability of clear-sky data in wet tropical regions (Maeda et al., 2016). Here~~,~~ we ~~found~~ find that, after correction with the MAIAC algorithm, EVI data from the Congo Basin's evergreen forest region do not present any significant difference between the two rainy seasons (Fig. 5b), and basin-wide MAIAC EVI appears to peak during SON rather than MAM (Fig. 4a). Furthermore, direct estimation of photosynthetic rates using SIF/PAR data reveals greater productivity and light use efficiency (LUE) in SON than MAM throughout the evergreen forest band (Fig. 5b) and the basin as a whole (Figs. 4b, S3). The misaligned seasonal peaks of SIF/PAR and ET_{wb} indicate that either a) water use efficiency (WUE) varies seasonally when generalized across the basin, resulting in higher MAM transpiration but lower MAM photosynthesis, or b) that the MAM peak in ET is primarily driven by direct evaporation from the canopy or land surface rather than transpiration.

4.2.1 Leaf age-related WUE variations

Leaf age offers a possible explanation for the variable WUE hypothesis. Studies of tropical trees have found that new leaves can take 1–2 months to reach peak photosynthetic capacity and WUE, and that both traits tend to decline as leaves reach 5–6 months old (Sobrado, 1994; Shirke, 2001). Leaf age has been linked to photosynthetic seasonality within the Amazon rainforest (Wu et al., 2016), although this effect has not been investigated in the Congo ~~basin~~Basin. Connecting the phenology of Congolese forests to basin-wide photosynthesis and transpiration must account for multiple broad ecoregions that span the equator and therefore face inverted seasonalities (Figs. 5, S2). In much of the deciduous woodlands of the northern (southern) basin, vegetation leaf flushing tends to begin 1–2 months prior to the onset of MAM (SON) rains and senescence begins around the end of the SON (MAM) rains, but both processes occur over the course of 1–2 months (Guan et al., 2014; Vinya et al., 2019). Likewise, microwave backscatter data from large areas of the Congo's evergreen forests imply ~~dry season leaf flushing likely occurs~~canopy biomass and/or water content peak during ~~DJF and~~ JJA and, to a lesser extent, DJF (Guan et al., 2013; Konings et al., 2017). But phenological observations from Gabon indicate that new leaf growth is suppressed during JJA and that the full mature-leaf tree canopies common in JJA contain an elevated fraction of senescing leaves, so dry season backscatter peaks in Congolese evergreen forests may not be attributable to widespread leaf flushing events (Bush, 2018). ~~Note, however, that~~Overall, the phenological synchronicity of leaf-out events appears to be low in the evergreen forests of central Africa (Couralet et al., 2013; Bush, 2018), so the magnitude and hydrologic effects of evergreen leaf flushing are probably smaller and more temporally distributed in the evergreen forests than in the deciduous woodlands of the basin.

After accounting for the different ecoregions within the Congo Basin, leaf age effects alone appear unable to explain the flipped seasonality of ET_{wb} in the two rainy seasons: although WUE increases as leaves mature, overall transpiration rates in tropical deciduous leaves remain high until they reach old age (Sobrado, 1994; Shirke, 2001). Thus, July–August leaf flushing of the southern deciduous woodlands, which far exceed the northern woodlands in area (Fig. S2), would most likely increase basin-wide transpiration alongside photosynthesis during SON. While our current understanding of regional phenology appears broadly consistent with remotely-sensed vegetation data, better field observations of phenology, leaf age,

and associated changes in stomatal conductance and productivity in the different ecosystems of the Congo ~~basin~~ Basin are needed to fully determine the role of vegetation in modulating ET seasonality.

4.2.2 VPD and temperature

Climatic conditions beyond precipitation could also contribute to the seasonal variations in WUE. For instance, high VPD reduces WUE by drawing more water from stomata per unit of carbon intake during transpiration. Basin-averaged VPD data from the ERA-Interim reanalysis do not indicate that MAM conditions are significantly less humid than SON conditions (Fig. 4e), suggesting seasonal VPD variations cannot explain the ~~flipped~~ swapped ET_{wb}–precipitation wet season magnitudes. But the uncertainties in reanalysis-based temperature and humidity data from tropical regions (Lorenz and Kunstmann, 2012; Brands et al., 2013) warrant an examination of the limited in-situ data available from within the Congo Basin. Observational VPD data from weather reports show that while ERA-Interim captures the shapes of seasonal VPD cycles fairly accurately, it fails to capture the magnitude of daytime VPDs in the evergreen rainforest (Fig. S1). Further examination of station and reanalysis data from within the evergreen forest region shows that rainforest VPD is slightly greater during MAM than SON (Figs. 5b, S1c–f), consistent with models based on historical pan evaporation data across the basin (Bultot, 1971) and historical atmospheric humidity data from within the equatorial rainforest (Lauer, 1989). However, because evergreen rainforest VPDs are generally low compared to other regions of the basin (Fig. 5) and are only slightly greater during MAM (Fig. S1c–f), VPD is not expected to be a significant driver of ET variations at basin-wide scales.

While basin-averaged T_a does not vary drastically throughout the year, T_s features a bimodal seasonality that peaks primarily in September and also from February to March (Fig. ~~S3~~S4). T_s can regulate ET via stomatal conductance, which tends to increase with leaf temperature to a point, although a wide range of sometimes-contradictory results have been published on this matter (Urban et al., 2017). In this case, the poor alignment of peak T_s and ET_{wb} values—taken in conjunction with the widespread stomatal closures known to occur in tropical forests during the hottest parts of the day (Fisher et al., 2006; Konings and Gentine, 2017; Konings et al., 2017)—indicate that other variables are more directly responsible for the high ET_{wb} observed during MAM.

4.2.3 Radiative fluxes

The magnitude and quality of radiative fluxes can drive the dynamics of ET_{wb} by influencing primary production as well as WUE. R_n and total PAR are both diminished in SON relative to MAM levels (Fig. 4c), which does not explain the SON peak in primary production observed in SIF/PAR and EVI data (Fig. 4a, b). However, greater R_n levels during MAM could decrease WUE by increasing water demand, thereby driving the high ET_{wb} levels observed in MAM.

~~Additionally~~In addition to the magnitude of the incoming radiative flux, the quality of PAR ~~beyond the flux's magnitude~~ could affect WUE and explain the apparent decoupling of productivity from irradiance levels and ET_{wb}. Prior studies have found that increasing PAR_{diff}/PAR can ~~increase~~ raise WUE and ~~light use efficiency (LUE)~~LUE in tropical savannahs and global forest canopies, including ~~in~~ an Amazonian tropical broadleaf stand (Alton et al., 2007; Kanniah et al., 2013).

Furthermore, total canopy ET has been found to decrease as the diffuse light fraction increases (Rocha et al., 2004). Philippon et al. (2019) examined diffuse and direct irradiance data from the Breathing Earth System Simulator (BESS; Ryu et al., 2018) and the Satellite Application Facility for Climate Monitoring (CM-SAF; Müller et al., 2015) and ~~find~~ found that the ratio of direct irradiance is often higher during MAM than in SON throughout much of the Congo Basin. The CERES data produce similar results: while PAR_{diff}/PAR peaks in May, ~~on average it is significantly lower during the MAM season than during SON. PAR_{diff}/PAR~~it remains low throughout March and April (the month when ET_{wb} peaks), and the greater total PAR flux in MAM is mostly attributable to greater PAR_{dir} (Fig. ~~S4~~S5). LUE (as approximated by PAR-normalized SIF) is greater during SON (Figs. 4b, 5), which is consistent with the presence of higher-quality radiation during the primary rainy season. After removing seasonal cycles and long-term trends, monthly mean SIF/PAR displays a strong negative correlation with mean PAR_{dir} but not with PAR_{diff}, indicating photosynthetic rates do not scale as well with increasing direct sunlight as with diffuse sunlight (Fig. ~~S5~~S6). These experiments suggest the quality of ~~insolation~~ irradiance during SON could allow for higher photosynthetic rates with lower ET than during MAM, especially since monthly PAR_{diff}/PAR in the Congo remains below 0.4 on average (Kanniah et al., 2013) and lower R_n corresponds to lower water demand (Philippon et al., 2019). Even if total PAR availability would favor a productivity peak in MAM, lower WUE and LUE could result in ~~plants transpiring all available water~~plants transpiring water at the highest possible rate without reaching the productivity levels achieved in SON. Thus ~~insolation~~ the quality of solar irradiance~~quality~~ potentially explains ET_{wb}'s imbalanced seasonality.

4.2.4 Terrestrial water storage

The availability of water in the rooting zone can modulate ET_{wb} by directly limiting transpiration during SON. In the Congo Basin, low average SIF values retrieved during both dry seasons even after normalizing for incident PAR imply that water availability could be limiting transpiration across all ecoregions (Figs. 4b, 5), warranting investigation of the terrestrial water dynamics of the basin.

As with other variables examined in this study, seasonal S dynamics at the basin scale are driven by the wet SON and dry JJA seasons experienced by the larger southern portion of the basin. Even though basin-wide P during MAM is significant, dS/dt (which measures groundwater within the rooting zone as well as in deeper reserves) remains much lower than its SON levels and only seems to recharge S enough to compensate for the slightly negative dS/dt values of January and February (Fig. 2), indicating that water reserves are largely saturated during MAM and undersaturated at the onset of SON when averaged across the basin (Fig. 4f). This hypothesis is consistent with prior soil moisture modeling efforts, which indicate that Congolese ecosystems south of the equator (i.e. most of the basin's area) feature low soil moisture as SON rains begin before maintaining high soil moisture and deeper water reserves through the end of the MAM rainy season (Pokam et al., 2012; Guan et al., 2014). Terrestrial water reserves are well-known to modulate productivity/ET throughout the basin (Saeed et al., 2013; Guan et al., 2014; Ndehedehe et al., 2018; Cuthbert et al., 2019), so depleted S during September and October could limit transpiration even after the dry season ends. This hypothesis is also consistent with recent findings that variability in soil moisture and groundwater are much more influential than variability in rainfall with regard to productivity anomalies within the Congo

Basin (Madani et al., 2020), making variations in plant-available soil moisture a plausible driver of the seasonal ET_{wb} imbalance when combined with the light quality impacts on WUE outlined in the previous section.

4.2.5 Direct canopy and soil evaporation

The WUE hypotheses explored above largely focus on the seasonality of transpiration, but seasonal variability in direct evaporation from forest canopies and the soil system could also potentially influence the seasonal cycle of ET_{wb}. As outlined above, R_n is lower in SON than during MAM (Fig. 4c), suggesting that there may simply be less energy driving direct evaporation of water from the land surface. As R_n and ET_{wb} both peak in March and high water content in the soil surface layer is apparently sustained throughout the rainy seasons (Guan et al., 2014), the conditions seem appropriate to drive increased direct evaporation during MAM. However, the higher proportion of nighttime rains during these months (Philippon et al., 2016) make this scenario less plausible, as recent rainfall would have more time to drip from the canopy to the soil surface and percolate to deeper soil levels. Additionally, a recent study of several climate models within the Congo Basin determined that soil and canopy evaporation rates are likely similar between the two wet seasons, and that the ET_{wb} seasonal imbalance is more likely due to increased transpiration during MAM (Crowhurst et al., 2020). More research is required to definitively characterize the role of direct evaporation in the seasonality of ET, but given the dominance of transpiration as the primary component of ET within the Congo Basin (Lian et al., 2018) and the conclusions of Crowhurst et al. (2020), we find it unlikely to be the main driver of ET_{wb}'s MAM peak.

Taken together, the analyses above suggest that the timing of peak ET rates in MAM rather than SON is primarily due to a combination of greater moisture availability and higher R_n during MAM, as well as the higher fraction of diffuse radiation during that season. The decoupled seasonal peaks of ET_{wb} and photosynthetic productivity also indicate that seasonal variations in WUE occur across the Congo Basin.

4.3 Comparison to global ET products

The ~~six~~ seven global ET models evaluated generally do not capture the ~~amplitudes~~ degrees of ~~interannual and seasonal~~seasonal and interannual variability displayed by ET_{wb} (Fig. 3, Table 3). Global ET product annual averages all fall within 10% of ET_{wb}'s, consistent with Weerasinghe et al. (2020)'s finding that global ET products can accurately capture the magnitude of long-term ET in the Congo Basin. Yet ~~Broadly speaking, FLUXCOM and to a lesser degree GLDAS Noah appear to lead global ET products in reproducing ET_{wb}. However, both of these products have significantly lower temporal standard deviations than ET_{wb} does. Indeed,~~ all ~~alternative~~ seven ET products have less temporal variability than ET_{wb}, ranging from only ~40% of ~~the~~ ET_{wb}'s variability (FLUXNET-MTE) to at most 80% of it (MERRA2). ~~-~~These metrics reflect not only the lack of seasonal variability in these models (Fig. 3), but also the fact that global ET models tend to repeat the same seasonal ET cycle every year with only minor ~~interannual variability~~variations. Although some products feature relatively accurate seasonal cycles, ~~(Fig. 3), ET_{wb} features~~ makes significant departures from its mean seasonal cycle in any given year (Fig. 1) that are not reflected in the ~~six~~ seven ET products evaluated here.

Broadly speaking, FLUXCOM and GLDAS-Noah appear to lead global ET products in reproducing ET_{wb} at monthly timescales—they feature the highest Taylor scores and Pearson coefficients, and also exhibit relatively large seasonal amplitudes (Table 3). However, both of these products still have significantly lower temporal standard deviations than ET_{wb} does and also display the largest overall biases from 2003–2011. After FLUXCOM and GLDAS-Noah, two primarily remote sensing-based products (MOD16A2 and GLEAM) achieve relatively high Taylor scores and Pearson coefficients, supporting previous reports that they approximate actual ET fairly well in tropical Africa (Schüttemeyer et al., 2007; Opoku-Duah et al., 2008; Andam-Akorful et al., 2015; Liu et al., 2016). Weerasinghe et al. (2020) found that FLUXNET-MTE and SSEBop exhibit very low long-term biases over the Congo Basin, but their low Taylor skill scores and standard deviations suggest a significant underestimation of month-to-month ET variability. Finally, ET from MERRA2 was found to possess the greatest temporal variability over the basin and, as a result, tied with FLUXCOM and GLDAS-Noah for the highest Taylor score; however, MERRA2 also produced the worst correlation coefficient and highest RMSE out of the seven global products.

Our results show some disagreements with the previous model comparison efforts of Liu et al. (2016). As part of a global water balance-based assessment of ET products, Liu et al. (2016) also compare ET_{wb} (estimated using a different approach; see below) to ET from GLEAM, FLUXNET-MTE, GLDAS-Noah~~OAH Version 2~~, and MERRA in the Congo Basin. However, in our calculation, the Taylor skill score of GLDAS-~~2.1~~Noah appears to far outperform its value in Liu et al. (2016), FLUXNET-MTE and MERRA2 both show modest improvements in their Taylor scores, and only GLEAM ~~v3.1a falls slightly short of its previous value~~falls into its previously-assigned score bin. These discrepancies were likely caused by a) the different study period used by Liu et al. (2016), which necessitated an extrapolation of GRACE data prior to 2002, b) the exclusive use of the GPCC Version 6 product to constrain P in their water balance models, and c) the use of different versions of the four datasets common to both Liu et al. (2016) and the present study. Nonetheless, comparison of these Taylor scores indicates that the most recent generation of ET products generally improved upon the previous generation ~~(GLEAM being the only partial exception)~~: FLUXCOM outperforms its predecessor, FLUXNET-MTE; GLDAS-~~NOAH~~ Noah Version 2.1 outperforms Version 2.0; and MERRA Version 2 improves upon MERRA Version 1's skill score.

~~Out of the six comparison products, the two remote sensing-based products diverge the most from ET_{wb}, despite being the most observationally-driven. While some previous studies have found MODIS-derived ET to approximate actual ET fairly well in nearby regions in West Africa (Schüttemeyer et al., 2007; Opoku-Duah et al., 2008; Andam-Akorful et al., 2015), the results of this comparison reinforce the value of ET_{wb} as a data-driven, independent estimate of a critical hydrological flux.~~

4.4 Effects of long-term climatic shifts on ET

From 2002–2016, no significant trend is detectable in the deseasonalized ET_{wb} data, nor in any of the other water balance component fluxes (Fig. 6). The lack of significant trends in water balance components over the fifteen-year study period is surprising given the numerous reports of declining precipitation in the Congo Basin, both in magnitude (Asefi-Najafabady and Saatchi, 2013; Diem et al., 2014; Zhou et al., 2014; Hua et al., 2016; Dezfuli, 2017) and ~~seasonality~~ in wet season duration (Jiang et al., 2019). However, the absence of a trend in P_{TC} does not ~~indicate~~ prove the absence of a longer-term drying trend

that began in the 20th century—rather, it probably results from our study period, which is shorter and generally more recent than those of the aforementioned studies~~, ; and~~ from our analysis of rainfall over all seasons rather than during certain three-month windows; and from the fact that rainfall declines mainly affect the northern portion of the basin (Zhou et al., 2014; Hua et al., 2016) whereas our study is dominated by the basin area south of the equator (Fig. S2). Indeed, careful examination of long-term precipitation ~~plots~~records from the literature reveals marked declines in rainfall during the 1990s and early 2000s that did not continue significantly into our 2002–2016 study period (Diem et al., 2014; Dezfuli, 2017; Hua et al., 2019). The lack of an interannual ET_{wb} trend is consistent with the recent findings of Weerasinghe et al. (2020).

The lack of long-term trends in ET_{wb} and EVI is ~~nevertheless surprising~~intriguing given the changes detectable in the other environmental variables (Figs. 7, ~~S6~~S7): PAR_{diff}, PAR_{dir}, R_n, and VPD all increase significantly from 2002–2016, ~~indicating~~ meaning the Congo Basin has become sunnier and less humid in recent years. While these findings should be viewed with caution because meteorological data are quite sparse in the basin during ~~this~~ the fifteen-year study period, the increasing VPD and irradiance trend~~s~~ ~~in ERA-Interim~~ are~~are~~ consistent with ~~projections of rising VPD~~long-term projections over the 21st century ~~-~~in CMIP5 models (Yuan et al., 2019; Zou et al., 2019). ~~-~~Sunnier and less humid conditions caused by increasing PAR, R_n, and VPD would typically lead to lower WUE in plants, which would in turn lead to increased ET and/or decreased EVI. Given the seasonal dependence of productivity and transpiration on irradiance levels (see Sect. 4.2.3), the apparent lack of a corresponding long-term relationship ~~indicates~~ suggests that some mechanism may be counteracting the biological impacts of rising irradiance and VPD.

Carbon fertilization offers one possible explanation for the lack of ET_{wb} and EVI trends. Rising VPD can indeed reduce the WUE of vegetation, but conversely, rising atmospheric CO_2 levels can increase WUE in tropical forests by catalyzing stomatal closure (De Kauwe et al., 2013; Keenan et al., 2013; Van Der Sleen et al., 2015). Ukkola and Prentice (2013)'s vegetation dynamics simulations yield a sizeable decrease in stomatal conductance between 1960 and 2000 in the Congo Basin, consistent with altered stomatal behavior from CO_2 fertilization and increasing VPD. ~~-~~Increasing PAR levels also could have helped support forest productivity rates as stomatal conductance declined, although~~but~~ the PAR data in Fig. ~~S6~~ S7 suggest a continual decrease in diffuse PAR fraction that could adversely affect the WUE and LUE of Congolese forests (Kanniah et al., 2013). In summary, even as VPD and irradiance have increased and driven up evaporative demand in plant stomata, the rising concentration of atmospheric CO_2 ~~has seemingly~~may have allowed the Congo's forests to lower stomatal conductance without significantly impacting growth or ET (Peñuelas et al., 2011; Van Der Sleen et al., 2015). But the effects of present and future carbon fertilization on WUE remain highly uncertain (Guerrieri et al., 2019), and a recent study of herbarium samples from Congolese evergreen forest trees found that while stomatal density has decreased from 1938 to 2013, inherent WUE has paradoxically decreased over the same period (Bauters et al., 2020). While the results of Bauters et al. (2020) pertain to a much longer time period and smaller spatial extent than our study and are thus difficult to compare here, they hint at the complexity of photosynthetic responses to environmental factors like VPD, CO_2 fertilization, temperature, and water availability, and suggest that Congolese forests may feature unique ecophysiological functions that warrant further study. ~~Thus~~Ultimately, ~~although~~ even if ET did not show any statistically-significant trends during our 2002~~–2015~~ 2016 study period

as a result of CO_2 fertilization, future ET rates could nevertheless start to change~~start declining~~ if the compensation between decreasing radiation quality and rising VPD on the one hand and increasing CO_2 on the other hand becomes imbalanced, or if long-term declines in precipitation continue.

4.5 Opportunities for further study

This study demonstrates the value in combining in-situ observations with remote sensing in data-sparse regions like the Congo Basin. However, there are clear limitations to the water-balance~~is~~ approach employed here that suggest several opportunities for further study of the region. For instance, applying the inverted water balance model at the basin scale masks differences in the magnitude and variability of ET across the diverse regions of the Congo Basin, but the availability of river discharge data from tributaries of the Congo River could allow for modeling of ET at the sub-basin scale (Alsdorf et al., 2016). Similarly, the monthly temporal resolution of the GRACE data prevents examination of diurnal and sub-monthly variations in ET. While GRACE data also represent a relatively short time span, the GRACE Follow-On (GRACE-FO) mission promises to extend the global *S* dataset well into the future. Ultimately, improved in-situ observations of hydrologic and climatic fluxes are necessary to understand the ecohydrology of central Africa in greater detail and at finer scales—eddy covariance towers, weather stations, and long-term phenological surveys would all be of great benefit to the growing field of research on the Congo Basin.

5 Conclusions

This study leverages several remotely-sensed and gauge-based precipitation datasets, river gauge data, and terrestrial water storage anomalies from GRACE to produce ET estimates for the Congo Basin in central Africa at the monthly timescale. This technique has been successfully applied to the Amazon Basin in recent years, but to the authors' knowledge it has not yet been used in the Congo Basin except as part of global-scale reviews of major river basins. The Congo Basin is greatly understudied despite its importance as one of the world's largest river basins and one of three major humid tropical forest regions, and quantification of basin-wide ET and its variability is imperative for understanding the basin's ~~basin's influence on regional and global climates~~climatic influence as well as its susceptibility to environmental disturbances. We find annual ET_{wb} to equal 117.2±3.5 cm/year, on average, from 2003–2015—well in line with many historical estimates of basin-wide ET.

Triple collocation was applied to determine the accuracy of *P* products over the sparsely-gauged Congo Basin, finding that the recently-developed NIC131-gridded dataset is the most accurate over our study period (RMSE of 0.65 cm/month). NIC131-gridded is followed by CHIRPS2 in terms of accuracy (RMSE of 0.93 cm/month), while three separate products that incorporate GPCC rain gauge data feature similar variability and RMSEs (1.60 to 1.67 cm/month). RMSEs from TC were also used to create a unified P_{TC} time series with a mean annual precipitation of 150.4±2.6 cm/year. A suite of global ET products is also evaluated versus ET_{wb}, with FLUXCOM and GLDAS-Noah Version 2.1 displaying the closest agreement with the

variability of ET_{wb} from 2003~~2~~–2011 and SSEBop most closely reproducing long-term mean ET. However, all ET models underestimated the seasonal and interannual variability of ET_{wb}.

In good agreement with existing literature, rainfall appears to exert a primary control on ET, but other environmental drivers appear to modulate ET and cause unexpected seasonal features, such as the MAM peak in ET recently explored by Crowhurst et al. (2020). Several possible causes for this MAM ET peak were investigated, but neither VPD, temperature, phenology, nor leaf age seasonalities could explain this MAM peak. Instead, the amount and quality of radiative energy and the availability of water in the terrestrial system appear to offer the most plausible explanations for the seasonal imbalance in peak ET_{wb}—higher diffuse PAR fractions and lower R_n during SON allow for higher WUE, while depleted terrestrial water stores limit the amount of water available for transpiration. On interannual timescales, VPD, R_n, and both direct and diffuse PAR increased from 2002–2016 while no trend was detectable in EVI and ET_{wb}, implying the rising concentration of atmospheric CO_2 may have~~has~~ compensated for the increasingly dry conditions facing the Congo Basin's forests. However, these effects may not remain balanced in a future of higher CO_2 levels, increased VPD and temperatures, and spreading deforestation within the basin.

Author contributions

AGK and MWB designed the study. MWB and GRQ retrieved the data. All authors analyzed the data. MWB prepared the manuscript with the assistance of AGK and GRQ.

Data availability

We provide our monthly basin-wide *P*, ET_{wb}, *dS/dt*, discharge, and other data online at http://doi.org/10.17605/OSF.IO/JPVMB.

Most of the original data products used in this study are freely available to the public: the HydroSHEDS basin boundary shapefile can be retrieved from https://hydrosheds.org/page/hydrobasins. PERSIANN-CDR data were accessed at http://dx.doi.org/10.7289/V51V5BWQ and CHIRPS2 data were downloaded from https://www.chc.ucsb.edu/data. The GPCC dataset was accessed at https://www.esrl.noaa.gov/psd/. GRACE data were retrieved from GRCTellus Land at http://grace.jpl.nasa.gov, and Congo River discharge data were downloaded from HYBAM at http://www.ore-hybam.org. FLUXNET-MTE and FLUXCOM were made available by the Max Planck Institute for Biogeochemistry; FLUXCOM may be accessed at http://fluxcom.org. GLEAM data were accessed at http://gleam.eu. SSEBop can be found at https://earlywarning.usgs.gov/fews/product/460. TRMM, MERRA2, and GLDAS-Noah data were provided by NASA GES DISC at https://disc.gsfc.nasa.gov/. CERES data were downloaded from https://ceres.larc.nasa.gov/order_data.php. ERA-Interim data were retrieved from the ECMWF at https://www.ecmwf.int/en/forecasts/datasets. MOD16A2 and MCD12C1 data

were downloaded from the USGS website at https://lpdaac.usgs.gov/products/mod16a2v006/ and https://lpdaac.usgs.gov/products/mcd12c1v006/, respectively, and AIRS data were downloaded from NASA's Giovanni web interface (https://giovanni.gsfc.nasa.gov/giovanni/). ASOS and MIDAS weather data were sourced from the UK Met Office's CEDA website at http://catalogue.ceda.ac.uk/uuid/220a65615218d5c9cc9e4785a3234bd0 and from Iowa State University's Iowa Environmental Mesonet site at https://mesonet.agron.iastate.edu/ASOS/.

Competing interests

The authors declare that they have no conflict of interest.

Acknowledgements

We gratefully acknowledge the researchers who provided their datasets and expertise for this study: A. Lyapustin and Y. Wang of NASA provided the MAIAC EVI data; S. Nicholson and D. Klotter of Florida State University provided their NIC131-gridded dataset; and J. Joiner of NASA provided the GOME-2 SIF data. C. Frankenberg of the California Institute of Technology graciously provided additional SIF data for comparison. We further thank two anonymous reviewers for helping us substantially improve this article. MWB was supported by a Stanford University Vice Provost for Undergraduate Education (VPUE) grant. This work was also supported by NASA Terrestrial Ecology award 80NSSC18K0715 through the New Investigator Program, by the NASA Carbon Cycle Science program, and by NOAA grant NA17OAR4310127.

References

Alemohammad, S. H., McColl, K. A., Konings, A. G., Entekhabi, D. and Stoffelen, A.: Characterization of precipitation product errors across the United States using multiplicative triple collocation, Hydrol. Earth Syst. Sci., 19, 3489–3503, https://doi.org/10.5194/hess-19-3489-2015, 2015.

Alemohammad, S. H., Fang, B., Konings, A. G., Aires, F., Green, J. K., Kolassa, J., Miralles, D., Prigent, C. and Gentine, P.: Water, Energy, and Carbon with Artificial Neural Networks (WECANN): a statistically based estimate of global surface turbulent fluxes and gross primary productivity using solar-induced fluorescence, Biogeosciences, 14, 4101–4124, https://doi.org/10.5194/bg-14-4101-2017, 2017.

Alsdorf, D., Beighley, E., Laraque, A., Lee, H., Tshimanga, R., O'Loughlin, F., Mahé, G., Dinga, B., Moukandi, G. and Spencer, R. G. M.: Opportunities for hydrologic research in the Congo Basin, Rev. Geophys., 54, 378–409, https://doi.org/10.1002/2016RG000517, 2016.

Alton, P. B., North, P. R. and Los, S. O.: The impact of diffuse sunlight on canopy light-use efficiency, gross photosynthetic product and net ecosystem exchange in three forest biomes, Glob. Chang. Biol., 13, 776–787, https://doi.org/10.1111/j.1365-

2486.2007.01316.x, 2007.

Andam-Akorful, S. A., Ferreira, V. G., Awange, J. L., Forootan, E. and He, X. F.: Multi-model and multi-sensor estimations of evapotranspiration over the Volta Basin, West Africa, Int. J. Climatol., 35, 3132–3145, https://doi.org/10.1002/joc.4198, 2015.

Asefi-Najafabady, S. and Saatchi, S.: Response of African humid tropical forests to recent rainfall anomalies., Philos. Trans. R. Soc. B, 368, 20120306, https://doi.org/10.1098/rstb.2012.0306, 2013.

Ashouri, H., Hsu, K. L., Sorooshian, S., Braithwaite, D. K., Knapp, K. R., Cecil, L. D., Nelson, B. R. and Prat, O. P.: PERSIANN-CDR: Daily precipitation climate data record from multisatellite observations for hydrological and climate studies, Bull. Am. Meteorol. Soc., 96, 69–83, https://doi.org/10.1175/BAMS-D-13-00068.1, 2015.

Awange, J. L., Ferreira, V. G., Forootan, E., Khandu, Andam-Akorful, S. A., Agutu, N. O. and He, X. F.: Uncertainties in remotely sensed precipitation data over Africa, Int. J. Climatol., 36, 303–323, https://doi.org/10.1002/joc.4346, 2016.

Baldocchi, D., Wilson, K., Valentini, R., Law, B., Munger, W., Davis, K., Wofsy, S., Pilegaard, K., Goldstein, A., Falge, E., Vesala, T., Hollinger, D., Running, S., Fuentes, J., Katul, G., Gu, L., Verma, S., Paw, K. T., Malhi, Y., Anthoni, P., Oechel, W., Schmid, H. P., Bernhofer, C., Meyers, T., Evans, R., Olson, R. and Lee, X.: FLUXNET: A New Tool to Study the Temporal and Spatial Variability of Ecosystem–Scale Carbon Dioxide, Water Vapor, and Energy Flux Densities, Bull. Am. Meteorol. Soc., 82, 2415–2434, https://doi.org/10.1175/1520-0477, 2002.

Balek, J., Ed.: Hydrology and Water Resources in Tropical Africa, Dev. Water Res., 8, Elsevier, New York., 1977.

Balek, J., Ed.: Hydrology and Water Resources in Tropical Regions, Dev. Water Res., 18, Elsevier, New York., 1983.

Batra, N., Yang, Y.-C. E., Choi, H. Il, Kumar, P., Cai, X. and De Fraiture, C.: Understanding Hydrological Cycle Dynamics Due to Changing Land Use and Land Cover: Congo Basin Case Study, in: IEEE International Geoscience and Remote Sensing Symposium 2008 (IGARSS 2008), Boston, July 7-11 2008, 491–494, https://doi.org/10.1109/IGARSS.2008.4780136, 2008.

Bauters, M., Meeus, S., Barthel, M., Stoffelen, P., De Deurwaerder, H. P. T., Meunier, F., Drake, T. W., Ponette, Q., Ebuy, J., Vermeir, P., Beeckman, H., Wyffels, F., Bodé, S., Verbeeck, H., Vandelook, F., & Boeckx, P.: Century-long apparent decrease in intrinsic water-use efficiency with no evidence of progressive nutrient limitation in African tropical forests, Glob. Change Biol., https://doi.org/10.1111/gcb.15145, 2020.

Beighley, R. E., Ray, R. L., He, Y., Lee, H., Schaller, L., Andreadis, K. M., Durand, M., Alsdorf, D. E. and Shum, C. K.: Comparing satellite derived precipitation datasets using the Hillslope River Routing (HRR) model in the Congo River Basin, Hydrol. Process., 25, 3216–3229, https://doi.org/10.1002/hyp.8045, 2011.

Bell, J. P., Tompkins, A. M., Bouka-Biona, C. and Sanda, I. S.: A process-based investigation into the impact of the Congo basin deforestation on surface climate, J. Geophys. Res. Atmos., 120, 5721–5739, https://doi.org/10.1002/2014JD022586, 2015.

Betbeder, J., Gond, V., Frappart, F., Baghdadi, N. N., Briant, G. and Bartholome, E.: Mapping of Central Africa Forested Wetlands Using Remote Sensing, IEEE J. Sel. Top. Appl. Earth Obs. Remote Sens., 7, 531–542, https://doi.org/10.1109/JSTARS.2013.2269733, 2014.

Bi, J., Myneni, R., Lyapustin, A., Wang, Y., Park, T., Chi, C., Yan, K. and Knyazikhin, Y.: Amazon forests' response to droughts: A perspective from the MAIAC product, Remote Sens., 8, 356, https://doi.org/10.3390/rs8040356, 2016.

Brands, S., Herrera, S., Fernández, J. and Gutiérrez, J. M.: How well do CMIP5 Earth System Models simulate present climate conditions in Europe and Africa?, Clim. Dyn., 41, 803–817, https://doi.org/10.1007/s00382-013-1742-8, 2013.

Bricquet, J.-P.: Transports en solution et en suspension par le bassin du fleuve Congo, in: Quatriemes Journees Hydrologiques de l'ORSTOM a Montpellier, 131–161, ORSTOM, Montpellier, 1988.

Bultot, F.: Atlas Climatique du Bassin Congolais, Deuxieme Partie: Les Composantes du Bilan d'Eau, L'Institut National pour L'Etude Agronomique du Congo (I.N.E.A.C.), Brussels, 1971.

Bush, E. R.: Tropical phenology in a time of change, PhD thesis, Faculty of Natural Sciences, University of Stirling, United Kingdom, 286 pp., 2018.

Bush, E. R., Jeffery, K., Bunnefeld, N., Tutin, C., Musgrave, R., Moussavou, G., Mihindou, V., Malhi, Y., Lehmann, D., Ndong, J. E., Makaga, L., and Abernethy, K.: Rare ground data confirm significant warming and drying in western equatorial Africa, PeerJ, 8, e8732, https://doi.org/10.7717/peerj.8732, 2020.

Camberlin, P., Barraud, G., Bigot, S., Dewitte, O., Makanzu Imwangana, F., Maki Mateso, J. C., Martiny, N., Monsieurs, E., Moron, V., Pellarin, T., Philippon, N., Sahani, M., & Samba, G.: Evaluation of remotely sensed rainfall products over Central Africa, Q. J. R. Meteorol. Soc., 145, 2115–2138, https://doi.org/10.1002/qj.3547, 2019.

Chishugi, J. B. and Alemaw, B. F.: The Hydrology of the Congo River Basin: A GIS-based Hydrological Water Balance Model, in: Proceedings of the 2009 World Environmental and Water Resources Congress: Great Rivers, Kansas City, MO, May 17-21 2009, 5864–5879, 2009.

Collins, J. M.: Temperature variability over Africa, J. Clim., 24, 3649–3666, https://doi.org/10.1175/2011JCLI3753.1, 2011.

Couralet, C., Van Den Bulcke, J., Ngoma, L. M., Van Acker, J. and Beeckman, H.: Phenology in functional groups of Central African rainforest trees, J. Trop. For. Sci., 25, 361–374, 2013.

Crowhurst, D. M., Dadson, S. J. and Washington, R.: Evaluation of Evaporation Climatology for the Congo Basin Wet Seasons in Eleven Global Climate Models, J. Geophys. Res. Atmos., 125, e2019JD030619, https://doi.org/10.1029/2019jd030619, 2020.

Crowley, J. W., Mitrovica, J. X., Bailey, R. C., Tamisiea, M. E. and Davis, J. L.: Land water storage within the Congo Basin inferred from GRACE satellite gravity data, Geophys. Res. Lett., 33, L19402, https://doi.org/10.1029/2006GL027070, 2006.

Cuthbert, M. O., Gleeson, T., Moosdorf, N., Befus, K. M., Schneider, A., Hartmann, J. and Lehner, B.: Global patterns and dynamics of climate–groundwater interactions, Nat. Clim. Chang., 9, 137–141, https://doi.org/10.1038/s41558-018-0386-4, 2019.

Dee, D. P., Uppala, S. M., Simmons, A. J., Berrisford, P., Poli, P., Kobayashi, S., Andrae, U., Balmaseda, M. A., Balsamo, G., Bauer, P., Bechtold, P., Beljaars, A. C. M., van de Berg, L., Bidlot, J., Bormann, N., Delsol, C., Dragani, R., Fuentes, M., Geer, A. J., Haimberger, L., Healy, S. B., Hersbach, H., Hólm, E. V., Isaksen, L., Kållberg, P., Köhler, M., Matricardi, M., Mcnally, A. P., Monge-Sanz, B. M., Morcrette, J. J., Park, B. K., Peubey, C., de Rosnay, P., Tavolato, C., Thépaut, J. N. and

Vitart, F.: The ERA-Interim reanalysis: Configuration and performance of the data assimilation system, Q. J. R. Meteorol. Soc., 137, 553–597, https://doi.org/10.1002/qj.828, 2011.

Dembélé, M. and Zwart, S. J.: Evaluation and comparison of satellite-based rainfall products in Burkina Faso, West Africa, Int. J. Remote Sens., 37, 3995–4014, https://doi.org/10.1080/01431161.2016.1207258, 2016.

Dezfuli, A.: Climate of Western and Central Equatorial Africa, in: Oxford Research Encyclopedia of Climate Science, Oxford University Press, Oxford, https://doi.org/10.1093/acrefore/9780190228620.013.511, 2017.

Diem, J. E., Ryan, S. J., Hartter, J. and Palace, M. W.: Satellite-based rainfall data reveal a recent drying trend in central equatorial Africa, Clim. Change, 126, 263–272, https://doi.org/10.1007/s10584-014-1217-x, 2014.

Doelling, D.: CERES SYN1DEG-MONTH HDF4 file - Edition 4A, NASA Langley Atmospheric Science Data Center DAAC, https://doi.org/10.5067/TERRA+AQUA/CERES/SYN1DEGMONTH_L3.004A, 2017.

Dong, J., Lei, F., & Wei, L.: Triple collocation based multi-source precipitation merging, Front. Water, 2, 1. https://doi.org/10.3389/frwa.2020.00001, 2020.

Dyer, E. L. E., Jones, D. B. A., Nusbaumer, J., Li, H., Collins, O., Vettoretti, G. and Noone, D.: Congo Basin precipitation: Assessing seasonality, regional interactions, and sources of moisture, J. Geophys. Res. Atmos., 122, 6882–6898, https://doi.org/10.1002/2016JD026240, 2017.

Van Der Ent, R. J. and Savenije, H. H. G.: Length and time scales of atmospheric moisture recycling, Atmos. Chem. Phys., 11, 1853–1863, https://doi.org/10.5194/acp-11-1853-2011, 2011.

Fisher, R. A., Williams, M., Do Vale, R. L., Da Costa, A. L. and Meir, P.: Evidence from Amazonian forests is consistent with isohydric control of leaf water potential, Plant, Cell Environ., 29, 151–165, https://doi.org/10.1111/j.1365-3040.2005.01407.x, 2006.

Friedl, M. and Sulla-Menashe, D.: MCD12C1 MODIS/Terra+Aqua Land Cover Type Yearly L3 Global 0.05Deg CMG V006, NASA Land Processes DAAC, https://doi.org/10.5067/MODIS/MCD12C1.006, 2015.

Funk, C., Peterson, P., Landsfeld, M., Pedreros, D., Verdin, J., Shukla, S., Husak, G., Rowland, J., Harrison, L., Hoell, A. and Michaelsen, J.: The climate hazards infrared precipitation with stations—a new environmental record for monitoring extremes, Sci. Data, 2, 150066, https://doi.org/10.1038/sdata.2015.66, 2015.

Gelaro, R., McCarty, W., Suárez, M. J., Todling, R., Molod, A., Takacs, L., Randles, C. A., Darmenov, A., Bosilovich, M. G., Reichle, R., Wargan, K., Coy, L., Cullather, R., Draper, C., Akella, S., Buchard, V., Conaty, A., da Silva, A. M., Gu, W., Kim, G. K., Koster, R., Lucchesi, R., Merkova, D., Nielsen, J. E., Partyka, G., Pawson, S., Putman, W., Rienecker, M., Schubert, S. D., Sienkiewicz, M. and Zhao, B.: The modern-era retrospective analysis for research and applications, version 2 (MERRA-2), J. Clim., 30, 5419–5454, https://doi.org/10.1175/JCLI-D-16-0758.1, 2017.

Guan, K., Wolf, A., Medvigy, D., Caylor, K. K., Pan, M. and Wood, E. F.: Seasonal coupling of canopy structure and function in African tropical forests and its environmental controls, Ecosphere, 4, 35, https://doi.org/10.1890/ES12-00232.1, 2013.

Guan, K., Wood, E. F., Medvigy, D., Kimball, J., Pan, M., Caylor, K. K., Sheffield, J., Xu, X. and Jones, M. O.: Terrestrial hydrological controls on land surface phenology of African savannas and woodlands, J. Geophys. Res. Biogeosciences, 119,

1652–1669, https://doi.org/10.1002/2013JG002572, 2014.

Guan, K., Pan, M., Li, H., Wolf, A., Wu, J., Medvigy, D., Caylor, K. K., Sheffield, J., Wood, E. F., Malhi, Y., Liang, M., Kimball, J. S., Saleska, S. R., Berry, J., Joiner, J. and Lyapustin, A. I.: Photosynthetic seasonality of global tropical forests constrained by hydroclimate, Nat. Geosci., 8, 284–289, https://doi.org/10.1038/ngeo2382, 2015.

Guerrieri, R., Belmecheri, S., Ollinger, S. V., Asbjornsen, H., Jennings, K., Xiao, J., Stocker, B. D., Martin, M., Hollinger, D. Y., Bracho-Garrillo, R., Clark, K., Dore, S., Kolb, T., William Munger, J., Novick, K. and Richardson, A. D.: Disentangling the role of photosynthesis and stomatal conductance on rising forest water-use efficiency, Proc. Natl. Acad. Sci. U. S. A., 116, 16909–16914, https://doi.org/10.1073/pnas.1905912116, 2019.

Hassan, A. and Jin, S.: Water storage changes and balances in Africa observed by GRACE and hydrologic models, Geod. Geodyn., 7, 39–49, https://doi.org/10.1016/j.geog.2016.03.002, 2016.

Hilker, T., Lyapustin, A. I., Tucker, C. J., Sellers, P. J., Hall, F. G. and Wang, Y.: Remote sensing of tropical ecosystems: Atmospheric correction and cloud masking matter, Remote Sens. Environ., 127, 370–384, https://doi.org/10.1016/j.rse.2012.08.035, 2012.

Hua, W., Zhou, L., Chen, H., Nicholson, S. E., Raghavendra, A. and Jiang, Y.: Possible causes of the Central Equatorial African long-term drought, Environ. Res. Lett., 11, 124002, https://doi.org/10.1088/1748-9326/11/12/124002, 2016.

Hua, W., Zhou, L., Nicholson, S. E., Chen, H. and Qin, M.: Assessing reanalysis data for understanding rainfall climatology and variability over Central Equatorial Africa, Clim. Dyn., ~~1–19~~53, 651–669, https://doi.org/10.1007/s00382-018-04604-0, 2019.

~~Huete, A., Didan, K., Miura, T., Rodriguez, E. P., Gao, X. and Ferreira, L. G.: Overview of the radiometric and biophysical performance of the MODIS vegetation indices, Remote Sens. Environ., 83, 195–213, 2002.~~

Huffman, G. J., Bolvin, D. T., Nelkin, E. J., Wolff, D. B., Adler, R. F., Gu, G., Hong, Y., Bowman, K. P. and Stocker, E. F.: The TRMM Multisatellite Precipitation Analysis (TMPA): Quasi-Global, Multiyear, Combined-Sensor Precipitation Estimates at Fine Scales, J. Hydrometeorol., 8, 38–55, https://doi.org/10.1175/JHM560.1, 2007.

James, R. and Washington, R.: Changes in African temperature and precipitation associated with degrees of global warming, Clim. Change, 117, 859–872, https://doi.org/10.1007/s10584-012-0581-7, 2013.

Jiang, Y., Zhou, L., Tucker, C. J., Raghavendra, A., Hua, W., Liu, Y. Y. and Joiner, J.: Widespread increase of boreal summer dry season length over the Congo rainforest, Nat. Clim. Chang., 9, 617–622, https://doi.org/10.1038/s41558-019-0512-y, 2019.

Joiner, J., Guanter, L., Lindstrot, R., Voigt, M., Vasilkov, A. P., Middleton, E. M., Huemmrich, K. F., Yoshida, Y. and Frankenberg, C.: Global monitoring of terrestrial chlorophyll fluorescence from moderate-spectral-resolution near-infrared satellite measurements: methodology, simulations, and application to GOME-2, Atmos. Meas. Tech., 6, 2803–2823, https://doi.org/10.5194/amt-6-2803-2013, 2013.

Jung, M., Reichstein, M., Margolis, H. A., Cescatti, A., Richardson, A. D., Arain, M. A., Arneth, A., Bernhofer, C., Bonal, D., Chen, J., Gianelle, D., Gobron, N., Kiely, G., Kutsch, W., Lasslop, G., Law, B. E., Lindroth, A., Merbold, L., Montagnani, L., Moors, E. J., Papale, D., Sottocornola, M., Vaccari, F. and Williams, C.: Global patterns of land-atmosphere fluxes of carbon

dioxide, latent heat, and sensible heat derived from eddy covariance, satellite, and meteorological observations, J. Geophys. Res. ~~Biogeosciences~~, 116, ~~1–16~~G00J07, https://doi.org/10.1029/2010JG001566, 2011.

Jung, M., Koirala, S., Weber, U., Ichii, K., Gans, F., Camps-Valls, G., Papale, D., Schwalm, C., Tramontana, G. and Reichstein, M.: The FLUXCOM ensemble of global land-atmosphere energy fluxes, Sci. Data, 6, 74, https://doi.org/10.1038/s41597-019-0076-8, 2019.

Kahn, B. H., Irion, F. W., Dang, V. T., Manning, E. M., Nasiri, S. L., Naud, C. M., Blaisdell, J. M., Schreier, M. M., Yue, Q., Bowman, K. W., Fetzer, E. J., Hulley, G. C., Liou, K. N., Lubin, D., Ou, S. C., Susskind, J., Takano, Y., Tian, B. and Worden, J. R.: The atmospheric infrared sounder version 6 cloud products, Atmos. Chem. Phys., 14, 399–426, https://doi.org/10.5194/acp-14-399-2014, 2014.

Kanniah, K. D., Beringer, J. and Hutley, L.: Exploring the link between clouds, radiation, and canopy productivity of tropical savannas, Agric. For. Meteorol., 182–183, 304–313, https://doi.org/10.1016/j.agrformet.2013.06.010, 2013.

De Kauwe, M. G., Medlyn, B. E., Zaehle, S., Walker, A. P., Dietze, M. C., Hickler, T., Jain, A. K., Luo, Y., Parton, W. J., Prentice, I. C., Smith, B., Thornton, P. E., Wang, S., Wang, Y. P., Wårlind, D., Weng, E., Crous, K. Y., Ellsworth, D. S., Hanson, P. J., Seok Kim, H., Warren, J. M., Oren, R. and Norby, R. J.: Forest water use and water use efficiency at elevated CO_2: A model-data intercomparison at two contrasting temperate forest FACE sites, Glob. Chang. Biol., 19, 1759–1779, https://doi.org/10.1111/gcb.12164, 2013.

Keenan, T. F., Hollinger, D. Y., Bohrer, G., Dragoni, D., Munger, J. W., Schmid, H. P. and Richardson, A. D.: Increase in forest water-use efficiency as atmospheric carbon dioxide concentrations rise, Nature, 499, 324–327, https://doi.org/10.1038/nature12291, 2013.

Konings, A. G. and Gentine, P.: Global variations in ecosystem-scale isohydricity, Glob. Chang. Biol., 23, 891–905, https://doi.org/10.1111/gcb.13389, 2017.

Konings, A. G., Yu, Y., Xu, L., Yang, Y., Schimel, D. S. and Saatchi, S. S.: Active microwave observations of diurnal and seasonal variations of canopy water content across the humid African tropical forests, Geophys. Res. Lett., 44, 2290–2299, https://doi.org/10.1002/2016GL072388, 2017.

Landerer, F. W. and Swenson, S. C.: Accuracy of scaled GRACE terrestrial water storage estimates, Water Resour. Res., 48, ~~1–11~~W04531, https://doi.org/10.1029/2011WR011453, 2012.

Landerer, F. W., Dickey, J. O. and Güntner, A.: Terrestrial water budget of the Eurasian pan-Arctic from GRACE satellite measurements during 2003-2009, J. Geophys. Res., 115, D23115, https://doi.org/10.1029/2010JD014584, 2010.

Laporte, N. T., Stabach, J. A., Grosch, R., Lin, T. S. and Goetz, S. J.: Expansion of industrial logging in Central Africa, Science, 316, 1451, https://doi.org/10.1126/science.1141057, 2007.

Lauer, W.: Climate and Weather, in: Tropical Rain Forest Ecosystems: Biogeographical and Ecological Studies, edited by H. Lieth and M. J. A. Werger, 7–53, Elsevier, New York., 1989.

Lee, H., Beighley, R. E., Alsdorf, D., Jung, H. C., Shum, C. K., Duan, J., Guo, J., Yamazaki, D. and Andreadis, K.: Characterization of terrestrial water dynamics in the Congo Basin using GRACE and satellite radar altimetry, Remote Sens.

Environ., 115, 3530–3538, https://doi.org/10.1016/j.rse.2011.08.015, 2011.

Lehner, B., Verdin, K. and Jarvis, A.: New global hydrography derived from spaceborne elevation data, Eos, 89, 93–95, https://doi.org/10.1029/2008EO100001, 2008.

Lian, X., Piao, S., Huntingford, C., Li, Y., Zeng, Z., Wang, X., Ciais, P., McVicar, T. R., Peng, S., Ottlé, C., Yang, H., Yang, Y., Zhang, Y. and Wang, T.: Partitioning global land evapotranspiration using CMIP5 models constrained by observations, Nat. Clim. Chang., 8, 640–646, https://doi.org/10.1038/s41558-018-0207-9, 2018.

Liu, W., Wang, L., Zhou, J., Li, Y., Sun, F., Fu, G., Li, X. and Sang, Y. F.: A worldwide evaluation of basin-scale evapotranspiration estimates against the water balance method, J. Hydrol., 538, 82–95, https://doi.org/10.1016/j.jhydrol.2016.04.006, 2016.

Loeb, N.: CERES Level 3B EBAF-Surface Terra+Aqua netCDF file - Edition 4.0, NASA Langley Atmospheric Science Data Center DAAC, https://doi.org/10.5067/TERRA+AQUA/CERES/EBAF-SURFACE_L3B004.0, 2017.

Lorenz, C. and Kunstmann, H.: The hydrological cycle in three state-of-the-art reanalyses: intercomparison and performance analysis, J. Hydrometeorol., 13, 1397–1420, https://doi.org/10.1175/JHM-D-11-088.1, 2012.

Lyapustin, A., Martonchik, J., Wang, Y., Laszlo, I., & Korkin, S.: Multiangle implementation of atmospheric correction (MAIAC): 1. Radiative transfer basis and look-up tables, J. Geophys. Res., 116, D03210, https://doi.org/10.1029/2010JD014985, 2011a.

Lyapustin, A., Wang, Y., Korkin, S. and Huang, D.: MODIS Collection 6 MAIAC algorithm, Atmos. Meas. Tech., 11, 5741–5765, https://doi.org/10.5194/amt-11-5741-2018, 2018.

Lyapustin, A. I., Wang, Y., Laszlo, I., Hilker, T., Hall, F. G., Sellers, P. J., Tucker, C. J. and Korkin, S. V.: Multi-angle implementation of atmospheric correction for MODIS (MAIAC): 3. Atmospheric correction, Remote Sens. Environ., 127, 385–393, https://doi.org/10.1016/j.rse.2012.09.002, 2012.

Lyapustin, A., Wang, Y., Laszlo, I., Kahn, R., Korkin, S., Remer, L., Levy, R., & Reid, J. S. (2011). Multiangle implementation of atmospheric correction (MAIAC): 2. Aerosol algorithm, J. Geophys. Res., 116, D03211, https://doi.org/10.1029/2010JD014986, 2011b.

Madani, N., Kimball, J. S., Jones, L. A., Parazoo, N. C., and Guan, K.: Global analysis of bioclimatic controls on ecosystem productivity using satellite observations of solar-induced chlorophyll fluorescence, Remote Sens., 9, 530, https://doi.org/10.3390/rs9060530, 2017.

Madani, N., Kimball, J. S., Parazoo, N. C., Ballantyne, A. P., Tagesson, T., Jones, L. A., Reichle, R. H., Palmer, P. I., Velicogna, I., Bloom, A. A., Saatchi, S., Liu, Z. and Geruo, A.: Below-surface water mediates the response of African forests to reduced rainfall, Environ. Res. Lett., 15, 034063, https://doi.org/10.1088/1748-9326/ab724a, 2020.

Maeda, E. E., Moura, Y. M., Wagner, F., Hilker, T., Lyapustin, A. I., Wang, Y., Chave, J., Mõttus, M., Aragão, L. E. O. C. and Shimabukuro, Y.: Consistency of vegetation index seasonality across the Amazon rainforest, Int. J. Appl. Earth Obs. Geoinf., 52, 42–53, https://doi.org/10.1016/j.jag.2016.05.005, 2016.

Maeda, E. E., Ma, X., Wagner, F. H., Kim, H., Oki, T., Eamus, D. and Huete, A.: Evapotranspiration seasonality across the

Amazon Basin, Earth Syst. Dyn., 8, 439–454, https://doi.org/10.5194/esd-8-439-2017, 2017.

Marshall, M., Funk, C. and Michaelsen, J.: Examining evapotranspiration trends in Africa, Clim. Dyn., 38, 1849–1865, https://doi.org/10.1007/s00382-012-1299-y, 2012.

Martens, B., Miralles, D. G., Lievens, H., Van Der Schalie, R., De Jeu, R. A. M., Fernández-Prieto, D., Beck, H. E., Dorigo, W. A. and Verhoest, N. E. C.: GLEAM v3: Satellite-based land evaporation and root-zone soil moisture, Geosci. Model Dev., 10, 1903–1925, https://doi.org/10.5194/gmd-10-1903-2017, 2017.

Matsuyama, H., Oki, T., Shinoda, M. and Masuda, K.: The seasonal change of the water budget in the Congo River Basin, J. Meteorol. Soc. Japan, 72, 281–299, 1994.

McColl, K. A., Vogelzang, J., Konings, A. G., Entekhabi, D., Piles, M. and Stoffelen, A.: Extended triple collocation: Estimating errors and correlation coefficients with respect to an unknown target, Geophys. Res. Lett., 41, 6229–6236, https://doi.org/10.1002/2014GL061322, 2014.

McCollum, J. R., Gruber, A. and Ba, M. B.: Discrepancy between gauges and satellite estimates of rainfall in equatorial Africa, J. Appl. Meteorol., 39, 666–679, https://doi.org/10.1175/1520-0450-39.5.666, 2000.

Mercado, L. M., Bellouin, N., Sitch, S., Boucher, O., Huntingford, C., Wild, M. and Cox, P. M.: Impact of changes in diffuse radiation on the global land carbon sink, Nature, 458, 1014–1017, https://doi.org/10.1038/nature07949, 2009.

Met Office: Met Office Integrated Data Archive System (MIDAS) Land and Marine Surface Station Data (1853-current), NCAS British Atmospheric Data Centre, available at: http://catalogue.ceda.ac.uk/uuid/220a65615218d5c9cc9e4785a3234bd0, 2012.

Miralles, D. G., Holmes, T. R. H., De Jeu, R. A. M., Gash, J. H., Meesters, A. G. C. A. and Dolman, A. J.: Global land-surface evaporation estimated from satellite-based observations, Hydrol. Earth Syst. Sci., 15, 453–469, https://doi.org/10.5194/hess-15-453-2011, 2011.

Mu, Q., Zhao, M. and Running, S. W.: MODIS Global Terrestrial Evapotranspiration (ET) Product (MOD16A2/A3): Algorithm Theoretical Basis Document, University of Montana, Missoula, MT, 55 pp., 2013.

Müller, R., Pfeifroth, U., Träger-Chatterjee, C., Trentmann, J. and Cremer, R.: Digging the METEOSAT treasure—3 decades of solar surface radiation, Remote Sens., 7, 8067–8101, https://doi.org/10.3390/rs70608067, 2015.

Munzimi, Y. A., Hansen, M. C., Adusei, B. and Senay, G. B.: Characterizing Congo basin rainfall and climate using Tropical Rainfall Measuring Mission (TRMM) satellite data and limited rain gauge ground observations, J. Appl. Meteorol. Climatol., 54, 541–555, https://doi.org/10.1175/JAMC-D-14-0052.1, 2015.

Ndehedehe, C. E., Okwuashi, O., Ferreira, V. G. and Agutu, N. O.: Exploring evapotranspiration dynamics over Sub-Sahara Africa (2000–2014), Environ. Monit. Assess., 190, 400, https://doi.org/10.1007/s10661-018-6780-6, 2018.

Nguyen, P., Ombadi, M., Sorooshian, S., Hsu, K., AghaKouchak, A., Brathwaite, D., Ashouri, H. and Thorstensen, A. R.: The PERSIANN family of global satellite precipitation data: a review and evaluation of products, Hydrol. Earth Syst. Sci., 22, 5801–5816, https://doi.org/10.5194/hess-2018-177, 2018.

Nicholson, S. E., Kim, J., Ba, M. B. and Lare, A. R.: The mean surface water balance over Africa and its interannual variability,

J. Clim., 10, 2981–3002, https://doi.org/10.1175/1520-0442(1997)010<2981:TMSWBO>2.0.CO;2, 1997.

Nicholson, S. E., Klotter, D., Dezfuli, A. K. and Zhou, L.: New Rainfall Datasets for the Congo Basin and Surrounding Regions, J. Hydrometeorol., 19, 1379–1396, https://doi.org/10.1175/JHM-D-18-0015.1, 2018.

Nicholson, S. E., Klotter, D., Zhou, L. and Hua, W.: Validation of Satellite Precipitation Estimates over the Congo Basin, J. Hydrometeorol., 20, 631–656, https://doi.org/10.1175/JHM-D-18-0118.1, 2019.

Nizinski, J. J., Galat, G. and Galat-Luong, A.: Water balance and sustainability of eucalyptus plantations in the Kouilou basin (Congo-Brazzaville), Russ. J. Ecol., 42, 305–314, https://doi.org/10.1134/S1067413611040126, 2011.

Nizinski, J. J., Galat, G. and Galat-Luong, A.: Actual evapotranspiration and canopy resistance measurement of the savannah in the Kouilou basin (Congo-Brazzaville), Russ. J. Ecol., 45, 359–366, https://doi.org/10.1134/S1067413614050191, 2014.

Oki, T., Musiake, K., Masuda, K. and Matsuyama, H.: Global runoff estimation by atmospheric water balance using ECMWF data set, in: Proceedings of the IAHS Yokohama Symposium: Hydrology of Warm Humid Regions, Yokohama, Japan, July 13-15 1993, 163–171, 1993.

Olivry, J. C., Bricquet, J. P. and Mahé, G.: Vers un appauvrissement durable des ressources en eau de l'Afrique humide?, in: Proceedings of the IAHS Yokohama Symposium: Hydrology of Warm Humid Regions, Yokohama, Japan, July 13-15 1993, 67–78, 1993.

Opoku-Duah, S., Donoghue, D. N. M. and Burt, T. P.: Intercomparison of evapotranspiration over the Savannah Volta Basin in West Africa using remote sensing data, Sensors, 8, 2736–2761, https://doi.org/10.3390/s8042736, 2008.

Pagán, B. R., Maes, W. H., Gentine, P., Martens, B., and Miralles, D. G.: Exploring the potential of satellite solar-induced fluorescence to constrain global transpiration estimates, Remote Sens., 11, 413, https://doi.org/10.3390/rs11040413, 2019.

Pan, M., Sahoo, A. K., Troy, T. J., Vinukollu, R. K., Sheffield, J. and Wood, A. E. F.: Multisource estimation of long-term terrestrial water budget for major global river basins, J. Clim., 25, 3191–3206, https://doi.org/10.1175/JCLI-D-11-00300.1, 2012.

Peñuelas, J., Canadell, J. G. and Ogaya, R.: Increased water-use efficiency during the 20th century did not translate into enhanced tree growth, Glob. Ecol. Biogeogr., 20, 597–608, https://doi.org/10.1111/j.1466-8238.2010.00608.x, 2011.

Philippon, N., de Lapparent, B., Gond, V., Sèze, G., Martiny, N., Camberlin, P., Cornu, G., Morel, B., Moron, V., Bigot, S., Brou, T. and Dubreuil, V.: Analysis of the diurnal cycles for a better understanding of the mean annual cycle of forests greenness in Central Africa, Agric. For. Meteorol., 223, 81–94, https://doi.org/10.1016/j.agrformet.2016.04.005, 2016.

Philippon, N., Cornu, G., Monteil, L., Gond, V., Moron, V., Pergaud, J., Sèze, G., Bigot, S., Camberlin, P., Doumenge, C., Fayolle, A. and Ngomanda, A.: The light-deficient climates of western Central African evergreen forests, Environ. Res. Lett., 14, 034007, https://doi.org/10.1088/1748-9326/aaf5d8, 2019.

Pinet, P. and Souriau, M.: Continental erosion and large-scale relief, Tectonics, 7, 563–582, https://doi.org/10.1029/TC007i003p00563, 1988.

Pokam, W. M., Djiotang, L. A. T. and Mkankam, F. K.: Atmospheric water vapor transport and recycling in Equatorial Central Africa through NCEP/NCAR reanalysis data, Clim. Dyn., 38, 1715–1729, https://doi.org/10.1007/s00382-011-1242-7, 2012.

Rocha, A. V., Su, H. B., Vogel, C. S., Schmid, H. P. and Curtis, P. S.: Photosynthetic and water use efficiency responses to diffuse radiation by an aspen-dominated northern hardwood forest, For. Sci., 50, 793–801, 2004.

Rodell, M., Famiglietti, J. S., Chen, J., Seneviratne, S. I., Viterbo, P., Holl, S. and Wilson, C. R.: Basin scale estimates of evapotranspiration using GRACE and other observations, Geophys. Res. Lett., 31, 10–13, https://doi.org/10.1029/2004GL020873, 2004a.

Rodell, M., Famiglietti, J. S., Wiese, D. N., Reager, J. T., Beaudoing, H. K., Landerer, F. W. and Lo, M. H.: Emerging trends in global freshwater availability, Nature, 557, 651–659, https://doi.org/10.1038/s41586-018-0123-1, 2018.

Rodell, M., Houser, P. R., Jambor, U., Gottschalck, J., Mitchell, K., Meng, C., Arsenault, K., Cosgrove, B., Radakovich, J., Bosilovich, M., Entin, J. K., Walker, J. P., Lohmann, D. and Toll, D.: The Global Land Data Assimilation System, Bull. Am. Meteorol. Soc., 85, 381–394, https://doi.org/10.1175/BAMS-85-3-381, 2004b.

Rodell, M., McWilliams, E. B., Famiglietti, J. S., Beaudoing, H. K. and Nigro, J.: Estimating evapotranspiration using an observation based terrestrial water budget, Hydrol. Process., 25, 4082–4092, https://doi.org/10.1002/hyp.8369, 2011.

Russell, G. L. and Miller, J. R.: Global River Runoff Calculated from a Global Atmospheric General Circulation Model, J. Hydrol., 117, 241–254, 1990.

Ryu, Y., Jiang, C., Kobayashi, H. and Detto, M.: MODIS-derived global land products of shortwave radiation and diffuse and total photosynthetically active radiation at 5 km resolution from 2000, Remote Sens. Environ., 204, 812–825, https://doi.org/10.1016/j.rse.2017.09.021, 2018.

Saeed, F., Haensler, A., Weber, T., Hagemann, S. and Jacob, D.: Representation of extreme precipitation events leading to opposite climate change signals over the Congo basin, Atmosphere-Basel, 4, 254–271, https://doi.org/10.3390/atmos4030254, 2013.

Sakumura, C., Bettadpur, S. and Bruinsma, S.: Ensemble prediction and intercomparison analysis of GRACE time-variable gravity field models, Geophys. Res. Lett., 41, 1389–1397, https://doi.org/10.1002/2013GL058632, 2014.

Schneider, U., Becker, A., Finger, P., Meyer-Christoffer, A., Rudolf, B. and Ziese, M.: GPCC Full Data Monthly Product Version 7.0 at 2.5°: Monthly Land-Surface Precipitation from Rain-Gauges built on GTS-based and Historic Data, Global Precipitation Climatology Centre (GPCC), https://doi.org/10.5676/DWD_GPCC/FD_M_V7_250, 2015.

Schüttemeyer, D., Schillings, C., Moene, A. F. and de Bruin, H. A. R.: Satellite-based actual evapotranspiration over drying semiarid terrain in West Africa, J. Appl. Meteorol. Climatol., 46, 97–111, https://doi.org/10.1175/JAM2444.1, 2007.

Senay, G. B., Bohms, S., Singh, R. K., Gowda, P. H., Velpuri, N. M., Alemu, H., Verdin, J. P.: Operational evapotranspiration mapping using remote sensing and weather datasets: a new paramaterization for the SSEB approach, J. Am. Water Resour. As., 49, 577–591, https://doi.org/10.1111/jawr.12057, 2013.

Shahin, M.: Evapotranspiration, in: Hydrology and Water Resources of Africa, 157–212, Springer Netherlands, Dordrecht, 1994.

Shem, W. O.: Biosphere-atmosphere interaction over the Congo Basin and its influence on the regional hydrological cycle, PhD thesis, School of Earth and Atmospheric Sciences, Georgia Institute of Technology, USA, 141 pp., 2006.

Shirke, P. A.: Leaf photosynthesis, dark respiration, and fluorescence as influenced by leaf age in an evergreen tree, *Prosopis juliflora*, Photosynthetica, 39, 305–311, https://doi.org/10.1023/A:1013761410734, 2001.

Van Der Sleen, P., Groenendijk, P., Vlam, M., Anten, N. P. R., Boom, A., Bongers, F., Pons, T. L., Terburg, G. and Zuidema, P. A.: No growth stimulation of tropical trees by 150 years of CO_2 fertilization but water-use efficiency increased, Nat. Geosci., 8, 24–28, https://doi.org/10.1038/ngeo2313, 2015.

Sobrado, M. A.: Leaf age effects on photosynthetic rate, transpiration rate and nitrogen content in a tropical dry forest, Physiol. Plant., 90, 210–215, https://doi.org/10.1111/j.1399-3054.1994.tb02213.x, 1994.

Sorí, R., Nieto, R., Vicente-Serrano, S. M., Drumond, A. and Gimeno, L.: A Lagrangian perspective of the hydrological cycle in the Congo River basin, Earth Syst. Dyn., 8, 653–675, https://doi.org/10.5194/esd-8-653-2017, 2017.

Stoffelen, A.: Toward the true near-surface wind speed: Error modeling and calibration using triple collocation, J. Geophys. Res. Ocean., 103, 7755–7766, https://doi.org/10.1029/97JC03180, 1998.

Swann, A. L. S. and Koven, C. D.: A Direct Estimate of the Seasonal Cycle of Evapotranspiration over the Amazon Basin, J. Hydrometeorol., 18, 2173–2185, https://doi.org/10.1175/JHM-D-17-0004.1, 2017.

Swenson, S. and Wahr, J.: Post-processing removal of correlated errors in GRACE data, Geophys. Res. Lett., 33, ~~1–4~~L08402, https://doi.org/10.1029/2005GL025285, 2006.

Swenson, S. C.: GRACE MONTHLY LAND WATER MASS GRIDS NETCDF RELEASE Ver. 5.0, NASA Physical Oceanography DAAC, https://doi.org/10.5067/TELND-NC005, 2012.

Tapley, B. D., Bettadpur, S., Ries, J. C., Thompson, P. F. and Watkins, M. M.: GRACE Measurements of Mass Variability in the Earth System, Science, 305, 503–505, https://doi.org/10.1126/science.1099192, 2004.

Taylor, K. E.: Summarizing multiple aspects of model performance in a single diagram, J. Geophys. Res., 106, 7183–7192, 2001.

Thiemig, V., Rojas, R., Zambrano-Bigiarini, M., Levizzani, V. and De Roo, A.: Validation of satellite-based precipitation products over sparsely gauged African river basins, J. Hydrometeorol., 13, 1760–1783, https://doi.org/10.1175/JHM-D-12-032.1, 2012.

Turubanova, S., Potapov, P. V., Tyukavina, A. and Hansen, M. C.: Ongoing primary forest loss in Brazil, Democratic Republic of the Congo, and Indonesia, Environ. Res. Lett., 13, 074028, https://doi.org/10.1088/1748-9326/aacd1c, 2018.

Ukkola, A. M. and Prentice, I. C.: A worldwide analysis of trends in water-balance evapotranspiration, Hydrol. Earth Syst. Sci., 17, 4177–4187, https://doi.org/10.5194/hess-17-4177-2013, 2013.

Urban, J., Ingwers, M. W., McGuire, M. A. and Teskey, R. O.: Increase in leaf temperature opens stomata and decouples net photosynthesis from stomatal conductance in *Pinus taeda* and *Populus deltoides x nigra*, J. Exp. Bot., 68, 1757–1767, https://doi.org/10.1093/jxb/erx052, 2017.

Verbesselt, J., Hyndman, R., Newnham, G. and Culvenor, D.: Detecting trend and seasonal changes in satellite image time series, Remote Sens. Environ., 114, 106–115, https://doi.org/10.1016/j.rse.2009.08.014, 2010a.

Verbesselt, J., Hyndman, R., Zeileis, A. and Culvenor, D.: Phenological change detection while accounting for abrupt and

gradual trends in satellite image time series, Remote Sens. Environ., 114, 2970–2980, https://doi.org/10.1016/j.rse.2010.08.003, 2010b.

Verbesselt, J., Zeileis, A. and Hyndman, R.: Breaks for Additive Season and Trend (BFAST), available at: http://bfast.r-forge.r-project.org, 2015.

Vinya, R., Malhi, Y., Brown, N. D., Fisher, J. B., Brodribb, T. and Aragão, L. E. O. C.: Seasonal changes in plant–water relations influence patterns of leaf display in Miombo woodlands: evidence of water conservative strategies, Tree Physiol., 39, 104–112, https://doi.org/10.1093/treephys/tpy062, 2019.

Wahr, J., Swenson, S. and Velicogna, I.: Accuracy of GRACE mass estimates, Geophys. Res. Lett., 33, ~~1–5~~L06401, https://doi.org/10.1029/2005GL025305, 2006.

Wan, Z., Zhang, K., Xue, X., Hong, Z., Hong, Y. and Gourley, J. J.: Water balance-based actual evapotranspiration reconstruction from ground and satellite observations over the conterminous United States, Water Resour. Res., 51, 6485–6499, https://doi.org/10.1002/2015WR017311, 2015.

Washington, R., James, R., Pearce, H., Pokam, W. M. and Moufouma-Okia, W.: Congo Basin rainfall climatology: can we believe the climate models?, Philos. Trans. R. Soc. B Biol. Sci., 368, 20120296~~1–7~~, https://doi.org/10.1098/rstb.2012.0296, 2013.

Weerasinghe, I., Bastiaanssen, W., Mul, M., Jia, L. and van Griensven, A.: Can we trust remote sensing evapotranspiration products over Africa?, Hydrol. Earth Syst. Sci., 24, 1565–1586, https://doi.org/10.5194/hess-24-1565-2020, 2020.

Wu, J., Albert, L. P., Lopes, A. P., Restrepo-Coupe, N., Hayek, M., Wiedemann, K. T., Guan, K., Stark, S. C., Christoffersen, B., Prohaska, N., Tavares, J. V., Marostica, S., Kobayashi, H., Ferreira, M. L., Campos, K. S., da Silva, R., Brando, P. M., Dye, D. G., Huxman, T. E., Huete, A. R., Nelson, B. W. and Saleska, S. R.: Leaf development and demography explain photosynthetic seasonality in Amazon evergreen forests, Science, 351, 972–976, https://doi.org/10.1126/science.aad5068, 2016.

Yin, X. and Gruber, A.: Validation of the abrupt change in GPCP precipitation in the Congo River Basin, Int. J. Climatol., 30, 110–119, https://doi.org/10.1002/joc.1875, 2010.

Yuan, W., Zheng, Y., Piao, S., Ciais, P., Lombardozzi, D., Wang, Y., Ryu, Y., Chen, G., Dong, W., Hu, Z., Jain, A. K., Jiang, C., Kato, E., Li, S., Lienert, S., Liu, S., Nabel, J. E. M. S., Qin, Z., Quine, T., Sitch, S., Smith, W. K., Wang, F., Wu, C., Xiao, Z. and Yang, S.: Increased atmospheric vapor pressure deficit reduces global vegetation growth, Sci. Adv., 5, ~~1–12~~eaax1396, https://doi.org/10.1126/sciadv.aax1396, 2019.

Zhang, K., Kimball, J. S. and Running, S. W.: A review of remote sensing based actual evapotranspiration estimation, Wiley Interdiscip. Rev. Water, 3, 834–853, https://doi.org/10.1002/wat2.1168, 2016.

Zhang, Y., Joiner, J., Gentine, P. and Zhou, S.: Reduced solar-induced chlorophyll fluorescence from GOME-2 during Amazon drought caused by dataset artifacts, Glob. Chang. Biol., 24, 2229–2230, https://doi.org/10.1111/gcb.14134, 2018.

Zhou, L., Tian, Y., Myneni, R. B., Ciais, P., Saatchi, S., Liu, Y. Y., Piao, S., Chen, H., Vermote, E. F., Song, C. and Hwang, T.: Widespread decline of Congo rainforest greenness in the past decade, Nature, 508, 86–90, https://doi.org/10.1038/nature13265, 2014.

Zou, L., Wang, L., Li, J., Lu, Y., Gong, W., and Niu, Y.: Global surface solar radiation and photovoltaic power from Coupled Model Intercomparison Project Phase 5 climate models, J. Clean. Prod., 224, 304–324, https://doi.org/10.1016/j.jclepro.2019.03.268, 2019.